

A Graph Multi-separator Problem for Image Segmentation

Jannik Irmair^{1,2}, Shengxian Zhao¹, Jannik Presberger¹, Bjoern Andres^{1,2,*}

¹*TU Dresden* ²*Center for Scalable Data Analytics and AI Dresden/Leipzig*

Abstract

We propose a novel abstraction of the image segmentation task in the form of a combinatorial optimization problem that we call the *multi-separator problem*. Feasible solutions indicate for every pixel whether it belongs to a segment or a segment separator, and indicate for pairs of pixels whether or not the pixels belong to the same segment. This is in contrast to the closely related lifted multicut problem where every pixel is associated to a segment and no pixel explicitly represents a separating structure. While the multi-separator problem is NP-hard, we identify two special cases for which it can be solved efficiently. Moreover, we define two local search algorithms for the general case and demonstrate their effectiveness in segmenting simulated volume images of foam cells and filaments.

Keywords: Graph separators, combinatorial optimization, image segmentation, complexity

Contents

1	Introduction	2
2	Related work	2
3	Multi-separator problem	4
3.1	Problem statement	5
3.2	Connection to the lifted multicut problem	5
3.3	Hardness	8
3.4	Attraction or repulsion only	9
3.5	Feasibility of partial assignments	11
3.6	Absolute dominant costs	12
4	Local search algorithms	14
4.1	Greedy Separator Shrinking	16
4.2	Greedy Separator Growing	17
5	Application to image segmentation	20
5.1	Volume images of simulated foams and filaments	20
5.2	Problem setup	23
5.3	Alternative	24
5.4	Metric	24
5.5	Experiments	25
5.6	Results	25
5.7	Observations	25
5.7.1	General observations	25

*Correspondence: bjoern.andres@tu-dresden.de

5.7.2	Specific observations for filaments	28
5.7.3	Specific observations for foam cells	28
6	Conclusion	30
A	Appendix	34
A.1	Volume image synthesis (details)	34
A.2	Detailed numerical results for renderings	35
A.3	Analysis of parameters of watershed algorithm	35

1 Introduction

Fundamental in the field of image analysis is the task of decomposing an image into distinct objects. Instances of this task differ with regard to the risk of making specific mistakes: False cuts are the dominant risk e.g. for volume images of intrinsically one-dimensional filaments (Figure 8). False joins are the dominant risk e.g. for volume images of intrinsically three-dimensional foam cells (Figure 9). Mathematical abstractions of the image segmentation task in the form of optimization problems, as well as algorithms for solving these problems, exactly or approximately, typically have parameters for balancing the risk of false cuts and false joins. Outstanding from these abstractions is the lifted multicut problem (cf. Section 2) in that it treats cuts and joins symmetrically and allows the practitioner to bias solutions toward cuts or joins explicitly. In the lifted multicut problem, every pixel is associated to an object and no pixel explicitly represents a structure separating these objects. This is suitable for applications in the field of computer vision where, typically, every pixel can be associated to an object and no pixel explicitly represents a separating structure.

As the first and major contribution of this work, we analyze theoretically a novel abstraction of the image segmentation task in the form of a combinatorial optimization problem that we call the *multi-separator problem*. Like in the lifted multicut problem, feasible solutions make explicit for pairs of pixels whether these pixels belong to the same or distinct objects, and these two cases are treated symmetrically. Also like in the lifted multicut problem, the number and size of segments is not constrained by the problem but is instead determined by its solutions. Unlike for the lifted multicut problem, feasible solutions distinguish between separated and separating pixels in the image. As the second and minor contribution of this work, we examine empirically the accuracy of the multi-separator problem as a model for segmenting objects that are separated by other objects, specifically, of foam cells or filaments that are separated by foam membranes or void. To this end, we define algorithms for finding locally optimal feasible solutions to the multi-separator problem efficiently, apply these to simulated volume images of foams and filaments, and report the accuracy of reconstructed foams or filaments defined by the output, along with absolute computation times.

Throughout this article, we abstract images as graphs whose nodes relate one-to-one to image pixels, whose edges connect adjacent pixels as depicted in Figure 1, and whose component-inducing node subsets model feasible segments of the image. Although these graphs are grid graphs, we define and discuss the multi-separator problem for arbitrary graphs, and we do not exploit the grid structure algorithmically.

The remainder of the article is organized as follows. In Section 2, we discuss related work. In Section 3, we define the multi-separator problem, analyze its complexity and establish a connection to the lifted multicut problem. In Section 4, we define algorithms for finding locally optimal feasible solutions efficiently. In Section 5, we examine the accuracy of the multi-separator problem as a model for segmenting synthetic volume images of simulated foams and filaments. In Section 6, we draw conclusions and discuss perspectives for future work.

2 Related work

A close connection exists, as we show by Theorems 1 and 2, between the multi-separator problem we define and the lifted multicut problem defined by Keuper et al. (2015) and discussed by Horňáková

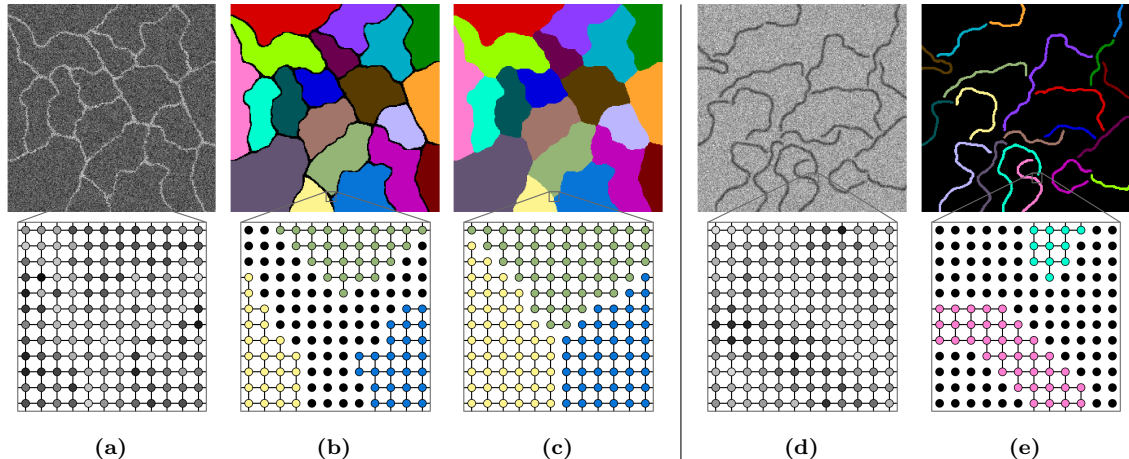


Figure 1: Depicted above are synthetic gray-scale images of foam cells, in (a), and filaments, in (d). Depicted in (b) and (e) in color are components of the pixel grid graphs of these image obtained by removing nodes (depicted in black). These nodes represent a separating structure that we call a *multi-separator* of the graph, and by which we treat the segmentation of foam cells and filaments analogously. This is in contrast to (c) where components of the pixel grid graph of the image (a) are obtained by removing edges, more specifically, a *multicut* of the graph, and no pixel represents a separating structure.

et al. (2017); Kardoost and Keuper (2018); Andres et al. (2023). Both problems are defined with respect to a graph $G = (V, E)$ and a set F of arbitrary node pairs. The feasible solutions to the lifted multicut problem relate one-to-one to the decompositions of the graph, i.e. all partitions of the node set into component-inducing subsets. These are precisely all ways of decomposing the graph by removing edges. In addition, the feasible solutions to the lifted multicut problem make explicit for all nodes pairs $\{u, v\} \in E \cup F$ whether u and v are in distinct components. By assigning a positive or negative cost to this decision, the objective function penalizes or rewards decompositions that have this property. No costs or constraints are imposed on the number or size of components. Instead, these properties are determined by the solutions. The lifted multicut problem has applications in the field of image analysis, notably to the tasks of image segmentation (Beier et al., 2017; Wolf et al., 2020; Lee et al., 2021), video segmentation (Keuper, 2017) and multiple object tracking (Tang et al., 2017). The multi-separator problem is similar in that the objective function assigns positive or negative costs to pairs of nodes being in distinct components. It is similar also in that no costs or constraints are imposed on the number or size of components and, instead, these properties are determined by the solutions. The multi-separator problem is different, however, in that its feasible solutions do not relate to all ways of decomposing the graph by removing edges but to all ways of separating the graph by removing nodes.

More fundamental is the multicut problem, i.e. the specialization of the lifted multicut problem with $F = \emptyset$, in which costs are assigned only to pairs of neighboring nodes (Chopra and Rao, 1993). The complexity and approximability of this problem and the closely related correlation clustering and coalition structure generation problems have been studied for signed graphs (Bansal et al., 2004), weighted graphs (Charikar et al., 2005; Demaine et al., 2006) and planar graphs (Voice et al., 2012; Bachrach et al., 2013; Klein et al., 2023). Connections to the task of image segmentation and algorithms are explored e.g. by Kappes et al. (2011); Andres et al. (2011); Yarkony et al. (2012); Beier et al. (2014); Kim et al. (2014); Zhang et al. (2014); Beier et al. (2015); Alush and Goldberger (2016); Kappes et al. (2016b,a); Kirillov et al. (2017); Kardoost and Keuper (2021).

Of particular interest for applications in image analysis are special cases of the multicut and lifted multicut problem that can be solved efficiently. As Wolf et al. (2020) show, the multicut problem can be solved efficiently for a cost pattern that we refer to here as absolute dominant costs. Their result implies that also the lifted multicut problem with absolute dominant costs and non-positive (i.e. cut-rewarding) costs for all non-neighboring node pairs can be solved efficiently.

The efficient algorithm by Wolf et al. (2020) is used e.g. by Lee et al. (2021) for segmenting volume images. In contrast, the lifted multicut problem with a non-negative (i.e. cut-penalizing) cost for even a single pair of non-neighboring nodes is NP-hard (Hornáková et al., 2017). This hampers applications of the lifted multicut problem to the task of segmenting volume images of filaments in which one would like to attribute positive costs to some pairs of non-neighboring nodes in order to prevent false cuts. Here, in this article, we show by Theorem 8: Unlike the lifted multicut problem, the multi-separator problem can be solved efficiently also for absolute dominant costs and non-negative costs for non-neighboring nodes.

An efficient technique for image segmentation by nodes separators is the computation of watersheds (Meyer, 1991; Vincent and Soille, 1991); see Roerdink and Meijster (2000) for a survey. Watersheds depend on weights attributed to individual nodes. Each component separated by watersheds corresponds to a local minimum of a node-weighted graph, or to a connected node set provided as additional input. In contrast, the multi-separator problem associates costs also with node pairs, and its solutions are not constrained to local optima. Watershed segmentation is canonical for images where a good initial estimate of components exists, like for images of foam cells. It is less canonical for images where such estimates are difficult, like for images of filaments. So far, fundamentally different models are used for reconstructing filaments, including (Rempfler et al., 2015; Shit et al., 2022; Türetken et al., 2016). In our experiments, we empirically compare feasible solutions to a multi-separator problem to watershed segmentations.

Toward more complex models for image segmentation by node separators, an NP-hard problem introduced and analyzed by Hornáková et al. (2020) is similar to the multi-separator problem in that it attributes unconstrained costs to pairs of nodes and in that its feasible solutions define components that are node-disjoint. It is different from the multi-separator problem in that the components defined by its feasible solutions are necessarily paths, and in that these components are not necessarily node-separated. An NP-hard problem introduced and analyzed by Nowozin and Lampert (2010) is similar to the multi-separator problem in that costs can penalize disconnectedness. It differs from the multi-separator problem in that feasible solutions define at most one component.

Graph separators have been studied also from a theoretical perspective. Structural results include Menger’s Theorem (Menger, 1927), the planar separator theorem (Lipton and Tarjan, 1979), and the observation that all minimal st -separators form a lattice (Escalante, 1972). An efficient algorithm for enumerating all minimal separators of a graph is by Berry et al. (2000). The problem of finding a partition of the node set of a graph into three sets A , B , C such that A and B are separated by C and such that $|C|$ is minimal subject to some constraints on $|A|$ and $|B|$ is studied by Balas and Souza (2005); Souza and Balas (2005); Didi Biha and Meurs (2011). This problem is NP-hard even for planar graphs (Fukuyama, 2006). The vertex k -cut problem asks for a minimum cardinality subset of nodes whose removal disconnects the graph into at least k components. Cornaz et al. (2018) show that this problem is NP-hard for $k \geq 3$. Exact algorithms for this problem are studied by Furini et al. (2020). For a given set of terminal nodes, the multi-terminal vertex separator problem consists in finding a subset of nodes whose removal disconnects the graph such that no two terminals are in the same component. This problem is studied by Garg et al. (2004); Cornaz et al. (2019); Magnouche et al. (2021). More loosely connected variants of the graph separator problem can be found in the referenced articles as well as in the articles referenced there. The multi-separator problem we propose here is different in that no costs or constraints are imposed on the number or size of components and, instead, these properties are determined by the solutions.

3 Multi-separator problem

In this section, we define the multi-separator problem as a combinatorial optimization problem over graphs and discuss its connection to the lifted multicut problem.

3.1 Problem statement

Let $G = (V, E)$ be a connected graph, let $S \subseteq V$ be a subset of nodes, and let $u, v \in V$ with $u \neq v$. We say u and v are *separated by S* if $u \in S$ or $v \in S$ or every uv -path in G passes through at least one node in S . Conversely, u and v are *not separated by S* if there exists a component in the subgraph of G induced by $V \setminus S$ that contains both u and v . In this article, we call every node subset $S \subseteq V$ a *multi-separator* or, abbreviating, just a *separator* of G . Examples are depicted in Figures 1b and 1e where the nodes of different colors are separated by the set of nodes depicted in black. Given an arbitrary set $F \subseteq \binom{V}{2}$ of node pairs, we let $F(S) \subseteq F$ denote the subset of those pairs that are separated by S .

Definition 1. Let $G = (V, E)$ be a connected graph, let $F \subseteq \binom{V}{2}$ be a set of node pairs called *interactions*, and let $c : V \cup F \rightarrow \mathbb{R}$ be called a *cost vector*. The *min-cost multi-separator* problem with respect to the graph G , the interactions F , and the cost vector c consists in finding a node subset $S \subseteq V$ called a *separator* so as to minimize the sum of the costs of the nodes in S plus the sum of the costs of those interactions $F(S) \subseteq F$ that are separated by S , i.e.

$$\min_{S \subseteq V} \sum_{v \in S} c_v + \sum_{f \in F(S)} c_f . \quad (\text{MSP})$$

We say an interaction $f \in F$ is *repulsive* if its associated costs c_f is negative, for in this case, the objective of (MSP) is decreased whenever f is separated. Analogously, we say f is *attractive* if the associated cost is positive. Likewise, we call a node $v \in V$ *repulsive* (*attractive*) whenever its associated cost c_v is negative (positive).

For any separator S , we define the characteristic vector $x^S : V \cup F \rightarrow \{0, 1\}$ such that $x_v^S = 1$ for $v \in S$, such that $x_v^S = 0$ for $v \in V \setminus S$, such that $x_f^S = 1$ for $f \in F(S)$, and such that $x_f^S = 0$ for $f \in F \setminus F(S)$. For the set of all such characteristic vectors, we write $\text{MS}(G, F) := \{x^S \mid S \subseteq V\}$. With this, (MSP) is written equivalently as

$$\min_{x \in \text{MS}(G, F)} \sum_{g \in V \cup F} x_g c_g . \quad (\text{MSP}')$$

3.2 Connection to the lifted multicut problem

The multi-separator problem (MSP) is closely related to the *lifted multicut problem* (Andres et al., 2023, Definition 5). In this section, we show that these problems are equally hard in the sense that solving either can be reduced in linear time to solving the other. In subsequent sections, we establish differences between these problems.

The *multicut problem* asks for a partition of the node set of a graph into component-inducing subsets such that the sum of the costs of the edges that straddle distinct components is minimized. The *lifted multicut problem* generalizes the multicut problem by assigning costs not only to edges of the graph but also to pairs of nodes that are not necessarily connected by an edge. Formally, the lifted multicut problem is defined as follows.

Definition 2. Let $G = (V, E)$ be a connected graph and let $\widehat{G} = (V, E \cup F)$ be an augmentation of G where $F \subseteq \binom{V}{2} \setminus E$ is called a set of (*additional*) *long-range edges*. A subset $M \subseteq E \cup F$ is called a *multicut of \widehat{G} lifted from G* if there exists a partition $\{\pi_1, \dots, \pi_n\}$ of V such that each π_i induces a component in G , and $M = \{\{u, v\} \in E \cup F \mid \forall i \in \{1, \dots, n\} : \{u, v\} \not\subseteq \pi_i\}$. Let $\text{LMC}(G, \widehat{G})$ denote the set of all multicuts of \widehat{G} lifted from G .

The *lifted multicut problem* with respect to the graph G , the augmented graph \widehat{G} and costs $c : E \cup F \rightarrow \mathbb{R}$ consists in finding a multicut of \widehat{G} lifted from G with minimal edge costs, i.e.

$$\min_{M \in \text{LMC}(G, \widehat{G})} \sum_{e \in M} c_e . \quad (\text{LMP})$$

The following two theorems state that the problems (MSP) and (LMP) can be reduced in linear time to one another. Examples of these reductions are depicted in Figure 2.

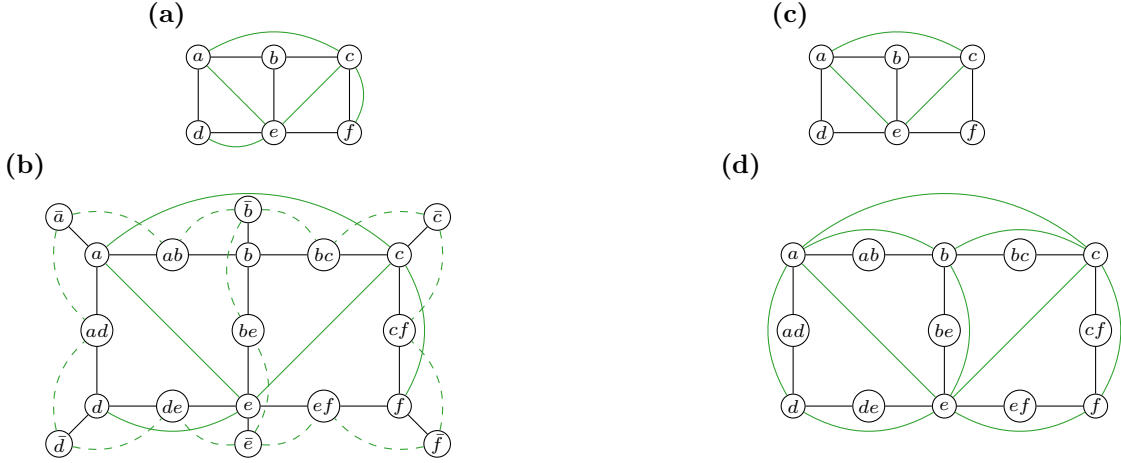


Figure 2: Depicted in (a) are a graph G (in black) and a set of interactions F (in green). Depicted in (b) are the corresponding auxiliary graph \tilde{G} (in black) and the set of long-range edges \tilde{F} (in green) that occur in the reduction of (MSP) to (LMP) in Theorem 1. The dashed edges have a high negative cost. This ensures that they are cut in any optimal solution. Depicted in (c) are a graph G (black edges) and an augmentation \hat{G} of G that contains the additional green edges. Depicted in (d) are the corresponding auxiliary graph \tilde{G} and the set of interactions \tilde{F} that occur in the reduction of (LMP) to (MSP) in Theorem 2.

Theorem 1. *The multi-separator problem (MSP) can be reduced to the lifted multicut problem (LMP) in linear time.*

Proof. To begin with, observe that a solution to the multi-separator problem can be represented as a solution to the lifted multicut problem by interpreting each node in the separator as a singleton component consisting of just this node. In the following, we construct an instance of (LMP) such that all relevant feasible solutions have this characteristic.

Let $G = (V, E)$ be a connected graph, let $F \subseteq \binom{V}{2}$ be a set of interactions, and let $c : V \cup F \rightarrow \mathbb{R}$ be a cost function that define an instance of (MSP). For $|V| = 1$, the multi-separator problem is trivial, so, from now on, we may assume $|V| \geq 2$. We construct an auxiliary graph $\tilde{G} = (\tilde{V}, \tilde{E})$, an augmentation $\hat{G} = (\tilde{V}, \tilde{E} \cup \tilde{F})$ of \tilde{G} , and costs $\bar{c} : \tilde{E} \cup \tilde{F} \rightarrow \mathbb{R}$ such that the optimal solutions of the instance of (MSP) with respect to G , F , and c correspond one-to-one to the optimal solutions of the instance of (LMP) with respect to \tilde{G} , \hat{G} , and \bar{c} . For each node $v \in V$, we consider the node v itself and a copy that we label \bar{v} . For each edge $\{v, w\} \in E$, we introduce an additional node that we label vw . For each $v \in V$, let $N_G(v) = \{w \in V \mid \{v, w\} \in E\}$ denote the set of neighbors of v in G , and let $\deg_G(v) = |N_G(v)|$ denote the degree of v in G . Altogether, we define nodes and edges as written below and as depicted in Figure 2 (a) and (b).

$$\begin{aligned}\tilde{V} &= V \cup \{\bar{v} \mid v \in V\} \cup \{vw \mid \{v, w\} \in E\} \\ \tilde{E} &= \{\{v, \bar{v}\} \mid v \in V\} \cup \{\{v, vw\} \mid v \in V, w \in N_G(v)\} \\ \tilde{F} &= F \cup \{\{\bar{v}, vw\} \mid v \in V, w \in N_G(v)\}\end{aligned}$$

With regard to the costs \bar{c} , we define $C = 1 + \sum_{g \in V \cup F} |c_g|$ and

$$\begin{aligned}\bar{c}_{\{v, \bar{v}\}} &= C \cdot \deg_G(v) & \forall v \in V \\ \bar{c}_{\{v, vw\}} &= C + \frac{c_v}{\deg_G(v)} & \forall v \in V \forall w \in N_G(v) \\ \bar{c}_{\{v, w\}} &= c_{\{v, w\}} & \forall \{v, w\} \in F \\ \bar{c}_{\{\bar{v}, vw\}} &= -C \cdot |V| & \forall v \in V \forall w \in N_G(v) .\end{aligned}$$

We show that there is a bijection ϕ from the feasible solutions of the instance of (MSP) with respect to G , F , and c onto those feasible solutions of the instance of (LMP) with respect to \tilde{G} ,

\widehat{G} , and \bar{c} that have cost less than $D = -2C|E|(|V| - 1) + C$. We remark that $-2C|E|(|V| - 1)$ is the cost of the lifted multicut that corresponds to the decomposition of \widehat{G} where the nodes \bar{v} for $v \in V$ are in singleton components and all other nodes form one large component (the degree sum formula yields $\sum_{v \in V} \deg_G(v) = 2|E|$).

Firstly, let $S \subseteq V$ be a feasible solution of (MSP) and let $C_S = \sum_{v \in S} c_v + \sum_{f \in F(S)} c_f$ be its cost. Then, by construction of \bar{G} and \widehat{G} , the set

$$\begin{aligned} M = \phi(S) = & \{ \{v, \bar{v}\} \mid v \in V \setminus S \} \\ & \cup \{ \{v, vw\} \mid v \in S, w \in N_G(v) \} \\ & \cup F(S) \\ & \cup \{ \{\bar{v}, vw\} \mid v \in V, w \in N_G(v) \} \end{aligned}$$

is a feasible multicut of \widehat{G} lifted from \bar{G} . By definition of the costs \bar{c} , the cost of M is $C_M = -2C|E|(|V| - 1) + C_S$. By definition of C follows $C_S < C$, and thus, $C_M < D$.

Secondly, let $M \subseteq \bar{E} \cup \bar{F}$ be any multicut of \widehat{G} lifted from \bar{G} with cost $C_M < D$. Since $C_M < D$ it must hold that $\{\bar{v}, vw\} \in M$ for all $v \in V$ and $w \in N_G(v)$. In the following, let $v \in V$ arbitrary but fixed. We show that either $\{v, \bar{v}\} \in M$ and $\{v, w\} \notin M$ for all $w \in N_G(v)$, or $\{v, \bar{v}\} \notin M$ and $\{v, w\} \in M$ for all $w \in N_G(v)$. (The two cases relate to the decisions of v being part or not of the separator in the solution to the corresponding multi-separator problem). If $\{v, \bar{v}\} \notin M$, then $\{v, vw\} \in M$ for all $w \in N_G(v)$, by the definition of lifted multicuts and $\{\bar{v}, vw\} \in M$. Otherwise, i.e. if $\{v, \bar{v}\} \in M$, then $\{v, vw\} \notin M$ for all $w \in N_G(v)$ since $C_M < D$. Together, we have that either $\{v, \bar{v}\}$ is cut and all other outgoing edges of v are not cut, or that $\{v, \bar{v}\}$ is not cut and all other outgoing edges of v are cut. Therefore, the separator $S = \{v \in V \mid \{v, \bar{v}\} \notin M\}$ is such that $M = \phi(S)$.

Together, we have shown that ϕ is a bijection from the set of feasible solutions of the instance of (MSP) to the set of feasible solutions of the instance of (LMP) with cost less than D . Moreover, the costs of feasible (MSP) solutions differ by the additive constant $-2C|E|(|V| - 1)$ from the costs of their images under ϕ . This concludes the proof that (MSP) can be reduced to (LMP). The time complexity of the reduction is linear in the size of the instance of (MSP), by construction. \square

Theorem 2. *The lifted multicut problem (LMP) can be reduced to the lifted multi-separator problem (MSP) in linear time.*

Proof. To begin with, observe that any solution to the lifted multicut problem can be represented as a solution to the multi-separator problem with respect to an auxiliary graph in which each edge of the original graph is replaced by two edges incident to an additional auxiliary node representative of the edge, namely as the separator consisting of precisely those auxiliary nodes whose corresponding edge is part of the lifted multicut. For an illustration, see Figure 2 (c) and (d).

More formally, let $G = (V, E)$ be a connected graph, let $\widehat{G} = (V, E \cup F)$ with $F \subseteq \binom{V}{2} \setminus E$ be an augmentation of G , and let $c : E \cup F \rightarrow \mathbb{R}$ be a cost function that define an instance of (LMP). Below, we construct an auxiliary graph $\bar{G} = (\bar{V}, \bar{E})$, a set of interactions $\bar{F} \subseteq \binom{\bar{V}}{2}$, and a cost function $\bar{c} : \bar{V} \cup \bar{F}$ such that the optimal solutions of the instance of (LMP) with respect to G , \widehat{G} , and c correspond one-to-one to the optimal solutions of the instance of (MSP) with respect to \bar{G} , \bar{F} , and \bar{c} . Specifically, we define

$$\begin{aligned} \bar{V} &= V \cup \{vw \mid \{v, w\} \in E\} \\ \bar{E} &= \{ \{v, vw\} \mid v \in V, \{v, w\} \in E \} \\ \bar{F} &= E \cup F . \end{aligned}$$

With regard to the costs \bar{c} , we define $C = 1 + \sum_{e \in E \cup F} |c_e|$ and

$$\begin{aligned} \bar{c}_v &= C \cdot |E| & \forall v \in V \\ \bar{c}_{vw} &= C & \forall \{v, w\} \in E \\ \bar{c}_{\{v, vw\}} &= 0 & \forall v \in V \ \forall \{v, w\} \in E \\ \bar{c}_e &= c_e - C & \forall e \in E \\ \bar{c}_f &= c_f & \forall f \in F . \end{aligned}$$

We establish the existence of a bijection ϕ from the feasible solutions of the instance of (LMP) with respect to G , \widehat{G} , and c onto those feasible solutions of the instance of (MSP) with respect to \bar{G} , \bar{F} , and \bar{c} that have cost less than C .

Firstly, let $M \subseteq E \cup F$ be a multicut of \widehat{G} lifted from G , and let $C_M = \sum_{e \in M} c_e$ be its cost. Then, the separator $S = \phi(M) = \{vw \mid \{v, w\} \in E \cap M\} \subseteq \bar{V}$ is a feasible solution of (MSP) with

$$\bar{F}(S) = M \cup \{\{v, vw\} \mid v \in V \wedge \{v, w\} \in E \cap M\} .$$

By the definition of \bar{c} , it has cost

$$C_S = \sum_{v \in S} \bar{c}_v + \sum_{f \in \bar{F}(S)} \bar{c}_f = \sum_{e \in M} \bar{c}_e = C_M . \quad (1)$$

Moreover, by definition of C , we have $C_S < C$.

Secondly, let $S \subseteq \bar{V}$ be a feasible solution to (MSP) with cost $C_S = \sum_{v \in S} \bar{c}_v + \sum_{f \in \bar{F}(S)} \bar{c}_f < C$. By the assumption that $C_S < C$ and the definition of \bar{c} , it follows that $v \notin S$ for all $v \in V$. Every $\{v, w\} \in E$ with $\{v, w\} \in \bar{F}(S)$ implies $vw \in S$, as otherwise, v and w would be connected by the path along the nodes v, vw, w , and thus, $\{v, w\} \notin \bar{F}(S)$, by definition of $\bar{F}(S)$. Conversely, by the assumption $C_S < C$, we have $\{v, w\} \in \bar{F}$ whenever $vw \in S$. Moreover, by the definitions of the set $\bar{F}(S)$ and lifted multicuts, $M = \bar{F}(S) \cap (E \cup F)$ is a multicut of \widehat{G} lifted from G . By construction: $\phi(M) = S$.

Together, we have shown that ϕ is a bijection from the set of feasible solution of the instance of (LMP) to the set of feasible solutions of the instance of (MSP) with cost less than C . Furthermore, by (1), the costs of feasible solutions related by ϕ are equal. Thus, finding an optimal solution to any of the two problems yields an optimal solution to the other. Moreover, the time complexity of the reduction is linear in the size of the instance of (LMP), by construction. \square

In spite of their mutual linear reducibility, there are differences between the lifted multicut problem, on the one hand, and the multi-separator problem, on the other hand: For $F = \emptyset$, the lifted multicut problem specializes to the multicut problem that is NP-hard, while the multi-separator problem specializes to the linear unconstrained binary optimization problem that can be solved in linear time. For $F \neq \emptyset$, we will extend this observation to specific cost functions in Theorem 8 and Theorem 9 below. Also for these specific cost functions, the lifted multicut problem is NP-hard, while the multi-separator problem can be solved efficiently.

3.3 Hardness

The reduction of the lifted multicut problem to the multi-separator problem in Theorem 2 implies several hardness results that we summarize below.

Corollary 1. *The multi-separator problem (MSP) is APX-hard.*

Proof. The reduction of (LMP) to (MSP) from Theorem 2 is approximation-preserving. This follows directly from the fact that the solutions that are mapped onto one another by the bijection ϕ have the same cost. Therefore, approximating (MSP) is at least as hard as approximating (LMP). This implies that (MSP) is APX-hard, as (LMP) is APX-hard (Andres et al., 2023). \square

Remark 1. In contrast to Corollary 1, the reduction of (MSP) to (LMP) from Theorem 1 is not approximation-preserving since the costs of two solutions that are mapped to one another differ by a large constant. Whether there exists an approximation-preserving reduction of (MSP) to (LMP) or whether approximating (MSP) is harder than approximating (LMP) is an open problem.

For planar graphs, Voice et al. (2012) and Bachrach et al. (2013) have shown independently that edge sum coalition structure generation is NP-hard. The edge sum graph coalition structure generation problem asks for a decomposition of a graph that maximizes the sum of the costs of those edges whose nodes are in the same component. Clearly, a decomposition maximizes the sum of the costs of those edges whose nodes are in the same component if and only if it minimizes the sum of the costs of those edges whose nodes are in distinct components. Thus, for any graph, finding an optimal edge sum graph coalition structure is equivalent to finding an optimal multicut. As the multicut problem is the special case of the lifted multicut problem without long-range edges, i.e. $F = \emptyset$, the reduction from Theorem 2 implies the following hardness result.

Corollary 2. *The multi-separator problem (MSP) is NP-hard even if the graph $(V, E \cup F)$ is planar.*

Proof. If $G = (V, E)$ is a planar graph, then the graph $(\bar{V}, \bar{E} \cup \bar{F})$ with \bar{V} , \bar{E} , and \bar{F} as in the reduction of (LMP) to (MSP) in Theorem 2 is also planar. \square

3.4 Attraction or repulsion only

In the following, we show: The multi-separator problem remains NP-hard for the special cases where all interactions are attractive or all interactions are repulsive. More specifically, we show that the multi-separator problem generalizes the quadratic unconstrained binary optimization (QUBO) problem, the node-weighted Steiner tree problem (Moss and Rabani, 2007) and the multi-terminal vertex separator problem (Cornaz et al., 2019).

Theorem 3. *Quadratic unconstrained binary optimization (QUBO) is equivalent to the special case of the multi-separator problem (MSP) with $E = F$.*

Proof. Let $n \in \mathbb{N}$, and $q_{ij} \in \mathbb{R}$ for all integers i and j such that $1 \leq i \leq j \leq n$. Then the quadratic unconstrained binary optimization problem with respect to coefficients q is defined as

$$\begin{aligned} \max \quad & \sum_{1 \leq i \leq j \leq n} q_{ij} x_{ij} & (\text{QUBO}) \\ \text{s.t.} \quad & x_{ii} \in \{0, 1\} & \forall i \in \{1, \dots, n\} \\ & x_{ij} = x_{ii} x_{jj} & \forall i \in \{1, \dots, n\} \forall j \in \{i+1, \dots, n\} . \end{aligned}$$

Let $G = (V, E)$ be the graph with $V = \{1, \dots, n\}$ and $E = \{\{i, j\} \mid q_{ij} \neq 0, 1 \leq i < j \leq n\}$, let $F = E$ be the set of interactions and let $c : V \cup F \rightarrow \mathbb{R}$ with $c_i = q_{ii}$ for $i \in V$ and $c_{\{i, j\}} = q_{ij}$ for $1 \leq i < j \leq n$ with $\{i, j\} \in F$. It is easy to see that the instance of (QUBO) with respect to q is equivalent to the instance of (MSP) with respect to G , F and c :

For all $x \in \text{MS}(G, F)$ and all $\{i, j\} \in F$, we have $x_{\{i, j\}} = 0 \Leftrightarrow x_i = x_j = 0$, which is equivalent to $1 - x_{\{i, j\}} = (1 - x_i)(1 - x_j)$. Therefore, the affine transformation $x \mapsto 1 - x$ is a bijection between the feasible solutions of the instance of (MSP) and the feasible solutions of the instance of (QUBO). Moreover, if x is a feasible solution to the instance of (QUBO) with cost $\sum_{1 \leq i \leq j \leq n} q_{ij} x_i x_j$, then $y = 1 - x$ is a feasible solution to the instance of (MSP) with cost

$$\sum_{g \in V \cup F} c_g y_g = \sum_{1 \leq i \leq n} c_i (1 - x_i) + \sum_{1 \leq i < j \leq n} c_{ij} (1 - x_i x_j) = \sum_{1 \leq i \leq j \leq n} q_{ij} - \sum_{1 \leq i \leq j \leq n} q_{ij} x_i x_j .$$

The two costs differ by sign and the additive constant term $\sum_{1 \leq i \leq j \leq n} q_{ij}$. Thus, the maximizers of the instance of (QUBO) are precisely the minimizers of the instance of (MSP), which concludes the proof. \square

Theorem 4. *The multi-separator problem (MSP) generalizes the node-weighted Steiner tree problem.*

Proof. Let $G = (V, E)$ be a connected graph, let $U \subseteq V$ be called a set of terminals, and let $w : V \rightarrow \mathbb{R}_{\geq 0}$ assign a non-negative weight to each node in G . The node-weighted Steiner tree problem with respect to G , U , and w consists in finding a node set $T \subseteq V$ with minimum cost $\sum_{v \in T} w_v$ such that the subgraph of G induced by T contains a component that contains U .

Let $U = \{u_1, \dots, u_k\}$ with $k = |U|$, and define interactions $F = \{\{u_1, u_2\}, \dots, \{u_1, u_k\}\}$. Furthermore, let $W := \sum_{v \in V} w_v$, and define costs $c : V \cup F \rightarrow \mathbb{R}$ with $c_v = -w_v$ for $v \in V$, and with $c_f = W + 1$ for $f \in F$. Now, consider the multi-separator problem (MSP) with respect to G , F , and c . By construction, the solutions to the Steiner tree problem relate one-to-one to the solutions of the multi-separator problem with non-positive cost: Every feasible solution $x \in \text{MS}(G, F)$ with non-positive cost, i.e. $\sum_{g \in V \cup F} c_g x_g \leq 0$, satisfies $x_f = 0$ for all $f \in F$. This implies that the subgraph of G induced by $x^{-1}(0)$ contains a component that contains U . Conversely, if T is a feasible solution to the Steiner tree problem then $x \in \{0, 1\}^{V \cup F}$ defined such that $x_v = 1$ for $v \notin T$ and such that $x_g = 0$ for $g \in T \cup F$ is a feasible solution to the multi-separator problem that has a non-positive cost.

Moreover,

$$\sum_{g \in V \cup F} c_g x_g = \sum_{v \in V \setminus T} c_v = - \sum_{v \in V \setminus T} w_v = \sum_{v \in T} w_v - W .$$

Consequently, the optimal solutions of the Steiner tree problem relate one-to-one to the optimal solutions of the multi-separator problem, which concludes the proof. \square

Theorem 5. *The multi-separator problem (MSP) generalizes the multi-terminal vertex separator problem.*

Proof. Let $G = (V, E)$ be a connected graph, let $U \subseteq V$ such that $\{u, v\} \notin E$ for $u, v \in U$ be called a set of terminals, and let $w : V \rightarrow \mathbb{R}_{\geq 0}$ assign a non-negative weight to each node in G . The multi-terminal vertex separator problem with respect to G , U and w consists in finding a node set $S \subseteq V \setminus U$ such that each pair $u, v \in U$, $u \neq v$ of terminals is separated by S and such that $\sum_{v \in S} w_v$ is minimal. The condition $\{u, v\} \notin E$ for $u, v \in U$ ensures that a feasible solution exists.

We define the set of interactions $F = \{\{u, v\} \mid u, v \in U, u \neq v\}$ as the set of all pairs of terminals. Furthermore, we define $W := \sum_{v \in V} w_v$ and costs $c : V \cup F$ such that $c_v = w_v$ for $v \in V \setminus U$, such that $c_v = W + 1$ for $v \in U$ and such that $c_f = -(W + 1)$ for $f \in F$. Now, consider the multi-separator problem (MSP) with respect to G , F and c . By construction, the solutions to the multi-terminal vertex separator problem correspond one-to-one to the solutions of the multi-separator problem with cost at most $-|F| \cdot (W + 1)$: Every feasible solution $x \in \text{MS}(G, F)$ with $\sum_{g \in V \cup F} c_g x_g \leq -|F|(W + 1)$ satisfies $x_f = 1$ for all $f \in F$ and satisfies $x_v = 0$ for all $v \in U$. This implies that any pair of terminals is separated by the node set $x^{-1}(1) \subseteq V \setminus U$, i.e. that $x^{-1}(1)$ is a feasible solution to the multi-terminal vertex separator problem. Conversely, if S is a feasible solution to the multi-terminal vertex separator problem, then $x \in \{0, 1\}^{V \cup F}$ defined such that $x_v = 0$ for $v \in V \setminus S$ and such that $x_g = 1$ for $g \in S \cup F$ is a feasible solution to the multi-separator problem with cost at most $-|F| \cdot (W + 1)$.

Moreover,

$$\sum_{g \in V \cup F} c_g x_g = -|F| \cdot (W + 1) + \sum_{v \in V \setminus U} c_v = -|F| \cdot (W + 1) + \sum_{v \in V \setminus U} w_v .$$

Consequently, the optimal solutions of the multi-terminal vertex separator problem relate one-to-one to the optimal solutions of the multi-separator problem, which concludes the proof. \square

It is well known that (QUBO) is NP-hard even if the costs of all quadratic terms are -1 (Barahona, 1982). Together with Theorem 3, this immediately implies the following hardness results for (MSP) with all repulsive interactions. The same result is obtained from the fact that the multi-terminal vertex separator problem is NP-hard (Garg et al., 1994), together with Theorem 5.

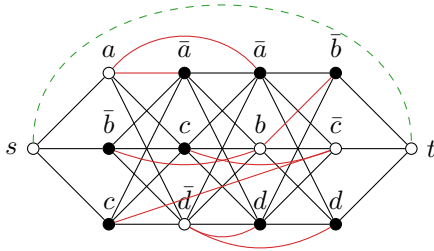


Figure 3: The 3-SAT problem can be reduced to deciding consistency for (MSP). For instance, the 3-SAT formula $(a \vee \bar{b} \vee c) \wedge (\bar{a} \vee c \vee \bar{d}) \wedge (\bar{a} \vee b \vee d) \wedge (\bar{b} \vee \bar{c} \vee d)$ is satisfiable if and only if there exists a separator S in the graph depicted above (solid edges) such that $\{s, t\}$ (green, dashed) is not separated by S and such that every pair $\{x, \bar{x}\}$ (red) for $x \in \{a, b, c, d\}$ is separated by S . This particular formula is satisfied, e.g., by the assignment $\{a, b, \bar{c}, \bar{d}\}$. The corresponding separator is depicted by the black nodes.

Corollary 3. *The multi-separator problem (MSP) is NP-hard even if $c_f = -1$ for all $f \in F$.*

Conversely, if the costs of all quadratic terms in the (QUBO) objective are positive, then the objective is supermodular and, thus, (QUBO) can be solved efficiently (Grötschel et al., 1981). In contrast, the multi-separator problem remains NP-hard even for all attractive interactions, due to Theorem 4:

Corollary 4. *The multi-separator problem (MSP) is NP-hard even if $c_f \geq 0$ for all $f \in F$ and $c_v \leq 0$ for all $v \in V$.*

Proof. In the proof of Theorem 4, the node-weighted Steiner tree problem is reduced to an instance that satisfies the conditions. Moreover, the node-weighted Steiner tree problem is a generalization of the edge-weighted Steiner tree problem (the edge-weighted version can be reduced to the node-weighted version by subdividing each edge and giving the new node its weight), which is well-known to be NP-hard (Karp, 1972). \square

3.5 Feasibility of partial assignments

The following theorem shows that the multi-separator problem is harder than quadratic unconstrained binary optimization, Steiner tree, and multi-terminal vertex separator, in the sense that deciding consistency is hard for the multi-separator problem and easy for the other problems. Here, deciding consistency refers to the problem of deciding whether a partial assignment to the variables of a problem has an extension to all variables of the problem that is a feasible solution. For the multi-separator problem, this problem is defined as follows.

Definition 3. Let $G = (V, E)$ be a connected graph, let $F \subseteq \binom{V}{2}$ be a set of interactions. A partial variable assignment $x : V \cup F \rightarrow \{0, 1, *\}$, where $*$ indicates no assignment, is called *consistent* with respect to G and F if and only if there exists $y \in \text{MS}(G, F)$ such that $x_g = y_g$ for all $g \in V \cup F$ with $x_g \in \{0, 1\}$. In that case, y is called a *feasible extension* of x .

Theorem 6. *Deciding consistency for the multi-separator problem (MSP) is NP-complete.*

Proof. Deciding consistency is in NP because any feasible extension serves as a certificate that can be verified in linear time. NP-hardness can be shown by reducing 3-SAT to deciding consistency for the multi-separator problem, exactly analogous to the proof of Theorem 1 of Horňáková et al. (2017). An example of this reduction is depicted in Figure 3. \square

The following lemma identifies two special cases in which consistency can be decided efficiently.

Lemma 1. *For the multi-separator problem (MSP), consistency can be decided in linear time if either $x_f \in \{0, *\}$ for all $f \in F$, or $x_f \in \{1, *\}$ for all $f \in F \setminus E$.*

Proof. Let $G = (V, E)$ be a connected graph, let $F \subseteq \binom{V}{2}$ be a set of interactions, and let $x : V \cup F \rightarrow \{0, 1, *\}$ be a partial assignment to the variables of the multi-separator problem with respect to G and F .

Firstly, suppose that $x_f \in \{0, *\}$ for all $f \in F$. Let $S = \{v \in V \mid x_v = 1\}$ be the set of nodes that is assigned to the separator by x . If there exists an interaction $f \in F$ with $x_f = 0$ such that f is separated by S , then x is clearly not consistent. Otherwise, $\{f \in F \mid x_f = 0\} \cap F(S) = \emptyset$. Now, let $y : V \cup F \rightarrow \{0, 1\}$ be the feasible solution that is induced by the separator S , i.e.

$$y_g = \begin{cases} 1 & \text{if } g \in S \cup F(S) \\ 0 & \text{otherwise} \end{cases}.$$

By construction, $y \in \text{MS}(G, F)$ and $x_g = y_g$ for all $g \in V \cup F$ with $x_g \in \{0, 1\}$, which implies that x is consistent. Therefore, consistency can be decided by the following algorithm: 1. Delete the nodes that are labeled 1 by x from the graph, 2. compute the connected components of the obtained graph, 3. check whether all interactions that are labeled 0 by x are contained in a connected component. Computing the connected component can be done in time $\mathcal{O}(|V| + |E|)$ by breadth-first search. The overall algorithm is linear in the size $|V| + |E| + |F|$ of the multi-separator problem instance.

Secondly, suppose that $x_f \in \{1, *\}$ for all $f \in F \setminus E$. Note: For any interaction that is an edge of G , i.e. $\{u, v\} \in F \cap E$, with $x_{\{u, v\}} = 0$, we need to have $x_u \neq 1 \neq x_v$ in order for x to be consistent. For the remainder of this proof, we may assume $x_u = x_v = 0$ for all $\{u, v\} \in F \cap E$ with $x_{\{u, v\}} = 0$. Let $S = \{v \in V \mid x_v \in \{1, *\}\}$ be the set of nodes that are assigned to the separator or do not have an assignment. If there exists an interaction $f \in F$ with $x_f = 1$ such that f is not separated by S , then x is clearly not consistent. Otherwise, it holds that $\{f \in F \mid x_f = 1\} \subseteq F(S)$. As before, let $y : V \cup F \rightarrow \{0, 1\}$ be the feasible solution induced by the separator S . Again, by construction, $y \in \text{MS}(G, F)$ and $x_g = y_g$ for all $g \in V \cup F$ with $x_g \in \{0, 1\}$, which implies that x is consistent. Similarly to above, consistency can be checked by the following algorithm: 0. Check if for all $\{u, v\} \in F \cap E$ with $x_{\{u, v\}} = 0$, it holds that $x_u \neq 1 \neq x_v$; otherwise, x is not consistent, 1. delete all nodes in $\{v \in V \mid x_v = 1 \text{ or } \nexists \{u, v\} \in F \cap E : x_{\{u, v\}} = 0\}$ from G , 2. compute the connected components of the obtained graph, 3. check whether all interaction that are labeled 1 by x are not contained in a connected component. This algorithm is also linear in the size of the instance of the multi-separator problem. \square

As shown in Theorems 3 to 5, quadratic unconstrained binary optimization, Steiner tree, and multi-terminal vertex separator can be modeled as special cases of the multi-separator problem. The three special cases all satisfy one of the two conditions of Lemma 1: The special case of (MSP) that is equivalent to quadratic unconstrained binary optimization (Theorem 3) satisfies $F \setminus E = \emptyset$, i.e. $x_f \in \{1, *\}$ for all $f \in F \setminus E$. The special cases of (MSP) used to model Steiner tree (Theorem 4) or multi-terminal vertex separator (Theorem 5) are such that either no interactions can be separated, i.e. $x_f = 0$ for all $f \in F$, or all interactions need to be separated, i.e. $x_f = 1$ for all $f \in F$. Thus, by Lemma 1, for quadratic unconstrained binary optimization, Steiner tree and multi-terminal vertex separator, consistency is efficiently decidable, whereas for the general multi-separator problem, it is NP-hard (Theorem 6).

3.6 Absolute dominant costs

In the remainder of this section, we analyze the multi-separator problem for a restricted class of cost functions. We begin with a brief motivation.

Suppose we are not interested in finding a feasible solution that minimizes a linear cost function but a feasible solution that avoids mistakes, with respect to a given order of severity. More specifically, we want to find a feasible solution by looking at the variables of a problem in a given order, avoiding to assign 0 to variables that we call *repulsive*, and avoiding to assign 1 to variables that we call *attractive*. For the (lifted) multicut problem, this preference problem is discussed in

detail by Wolf et al. (2020). For the multi-separator problem (MSP), this preference problem is discussed below.

Given a strict order $<$ on the set $V \cup F$ of variables, and given a bipartition $\{A, R\}$ of the set $V \cup F$ of variables, we refer to the variables in A as *attractive* and refer to the variables in R as *repulsive*. For any feasible solutions $x, y \in \text{MS}(G, F)$ with $x \neq y$, and for the smallest (with respect to $<$) variable g with $x_g \neq y_g$, we *prefer* x over y , written as $x \prec y$, if both $g \in A$ and $x_g = 0$, or if both $g \in R$ and $x_g = 1$. Otherwise, we prefer y over x , written as $y \prec x$. According to this definition, preference \prec is a strict order on the set of all feasible solutions. The *preferred multi-separator problem* consists in finding the feasible solution that is preferred over all other feasible solutions. This problem can be modeled as a (MSP) with a specific cost function:

Definition 4 (Compare Wolf et al. (2020, Equation (8))). A cost function $c : V \cup F \rightarrow \mathbb{R}$ is called *absolute dominant* if

$$|c_g| > \sum_{g' \in V \cup F, |c_{g'}| < |c_g|} |c_{g'}| \quad \forall g \in V \cup F . \quad (2)$$

Given an order g_1, \dots, g_n and a partition $\{A, R\}$ of $V \cup F$ into attractive and repulsive variables, we can define absolute dominant costs as

$$c_{g_i} = \begin{cases} 2^{n-i} & \text{if } g_i \in A \\ -2^{n-i} & \text{if } g_i \in R \end{cases} \quad \forall i \in \{1, \dots, n\} . \quad (3)$$

Now, the solutions to the preferred multi-separator problem with respect to $\{A, R\}$ and g_1, \dots, g_n are precisely the solutions to the (MSP) with respect to the costs c (Wolf et al., 2020).

As a direct consequence of Theorem 6, we obtain the following hardness result.

Theorem 7. *The multi-separator problem (MSP) is NP-hard even for absolute dominant costs.*

Proof. We show NP-hardness by reducing the problem of deciding consistency for (MSP) to solving (MSP) for absolute dominant costs.

To this end, let $x : V \cup F \rightarrow \{0, 1, *\}$ be a partial variable assignment for a given (MSP) instance with graph $G = (V, E)$ and interactions $F \subseteq \binom{V}{2}$. Let $n = |V \cup F|$, let $k = |\{g \in V \cup F \mid x_g \in \{0, 1\}\}|$ be the number of labeled variables, and let g_1, \dots, g_n be an enumeration of the variables $V \cup F$ such that $x_{g_i} \in \{0, 1\}$ for $i \in \{1, \dots, k\}$. Furthermore, let $A = \{g \in V \cup F \mid x_g = 0\}$ and $R = (V \cup F) \setminus A$. Now, let c be defined as in (3). Observe that x is consistent if and only if the optimal solution of the multi-separator problem with respect to costs c has a value that is at most $-\sum_{i=1}^k x_{e_i} 2^{n-i}$. \square

In contrast to the hardness result above, for both special cases that either all interactions are non-repulsive or all interactions are non-attractive, the multi-separator problem with absolute dominant costs can be solved efficiently:

Theorem 8. *The multi-separator problem (MSP) can be solved efficiently for absolute dominant costs if either $c_f \leq 0$ for all $f \in F \setminus E$ or $c_f \geq 0$ for all $f \in F$.*

Proof. We describe an algorithm that computes the optimal solution for the multi-separator problem with absolute dominant costs. This algorithm involves deciding consistency (cf. Section 3.5) and is therefore not a polynomial time algorithm in general. However, it is designed such that under the condition that either $c_f \leq 0$ for all $f \in F \setminus E$ or $c_f \geq 0$ for all $f \in F$, the consistency problems that need to be solved can be solved efficiently, by Lemma 1.

Let $x : V \cup F \rightarrow \{0, 1, *\}$ be a partial variable assignment. The algorithm starts with all variables being unassigned, i.e. $x_g = *$ for all $g \in V \cup F$. Clearly, x is consistent. Now, the algorithm iterates over all variables $g \in V \cup F$ in descending order of their absolute cost. In each iteration, the algorithm assigns the variable x_g to 0 if $c_g > 0$ and to 1 if $c_g \leq 0$. If by assigning the variable x_g to 0 or 1, x is no longer consistent, this assignment is revoked, i.e. $x_g = *$. We observe that, if x with $x_g = 0$ ($x_g = 1$) is not consistent, then it must hold that all consistent extensions

$y \in \text{MS}(G, F)$ of x with $x_g = *$ satisfy $y_g = 1$ ($y_g = 0$). After iterating over all variables, x is a consistent partial variable assignment that has exactly one consistent extension y , by the above observation. This consistent extension y is an optimal solution to the problem by the following argument: Suppose there exists a feasible solution y' with a strictly smaller cost. Let $g \in V \cup F$ be the variable with the largest absolute cost with $y_g \neq y'_g$. By the definition of absolute dominant costs (2) and the assumption that the cost of y' is smaller than the cost of y , it must hold that $c_g < 0$ if $y'_g = 1$ and $c_g > 0$ if $y'_g = 0$. Now, let $x : V \cup F \rightarrow \{0, 1, *\}$ be the partial variable assignment such that $x_{g'} = y'_{g'}$ for all $g' \in V \cup F$ with $|c_{g'}| \geq |c_g|$, and such that $x_{g'} = *$ for all $g' \in V \cup F$ with $|c_{g'}| < |c_g|$. If x was consistent, then the algorithm would have assigned the variable g to y'_g . This is in contradiction to $y_g \neq y'_g$. Thus, y is optimal.

The algorithm consists of $|V| + |F|$ iterations. In each iteration, it needs to be decided if the partial assignment x is consistent. By the design of the algorithm and the assumption that either $c_f \leq 0$ for all $f \in F \setminus E$ or $c_f \geq 0$ for all $f \in F$, the partial assignment satisfies one of the conditions of Lemma 1 (if $c_f \leq 0$ for all $f \in F \setminus E$, then $x_f \in \{1, *\}$ for all $f \in F \setminus E$. If $c_f \geq 0$ for all $f \in F$, then $x_f \in \{0, *\}$ for all $f \in F$). Therefore, consistency can be decided in linear time. Overall, the algorithm has a time complexity of $\mathcal{O}(n^2)$ with $n = |V| + |E| + |F|$ the size of the instance of the problem. \square

Remark 2. For absolute dominant costs and non-positive costs for all non-neighboring node pairs (i.e. $c_f \leq 0$ for all $f \in F \setminus E$), the algorithm described in the proof of Theorem 8 is similar to the Mutex-Watershed algorithm of Wolf et al. (2020). The Mutex-Watershed algorithm solves the lifted multicut problem efficiently for absolute dominant costs with all non-positive costs for all non-neighboring node pairs.

The fact that the multi-separator problem can be solved efficiently also for absolute dominant costs and *non-negative* costs for all interactions is a key difference to the lifted multicut problem that is NP-hard even for absolute dominant costs and non-negative costs for all non-neighboring node pairs:

Theorem 9. *The lifted multicut problem (LMP) with respect to a connected graph $G = (V, E)$, an augmented graph $\widehat{G} = (V, E \cup F)$ and absolute dominant edge costs $c : E \cup F \rightarrow \mathbb{R}$ with $c_e \leq 0$ for $e \in E$ and $c_f \geq 0$ for $f \in F$ is NP-hard.*

Proof. By Theorem 1 of Hornáková et al. (2017), deciding consistency of a partially labeled lifted multicut is NP-hard. Similarly to the proof of Theorem 7, we show that deciding consistency of a partially labeled lifted multicut can be reduced to solving the lifted multicut problem with respect to costs constrained as in Theorem 9.

Let $x : E \cup F \rightarrow \{0, 1, *\}$ be a partially labeled lifted multicut. Without loss of generality, we may assume $x^{-1}(0) \subseteq F$ and $x^{-1}(1) \subseteq E$ by the following arguments. If there was an edge $e \in E$ with $x_e = 0$, we would contract the edge e in G and \widehat{G} and consider the consistency problem with respect to the contracted graphs. If there was an edge $f \in F$ with $x_f = 1$, we would delete it from F and add it to E without altering the consistency problem.

Now, the claim follows analogously to the proof of Theorem 7. \square

4 Local search algorithms

In this section, we define two efficient local search algorithms for the multi-separator problem. Our main motivation for studying efficient algorithms that do not necessarily find optimal solutions comes from the task of segmenting volume images with voxel grid graphs with tens of millions of nodes (Figure 13).

One approach to defining efficient local search algorithms would be to map instances of the multi-separator problem to instances of the lifted multicut problem, as in the proof of Theorem 1, apply known local search algorithms to these, and construct feasible solutions from the output. This approach is hampered, however, by the fact that local search algorithms for the lifted multicut

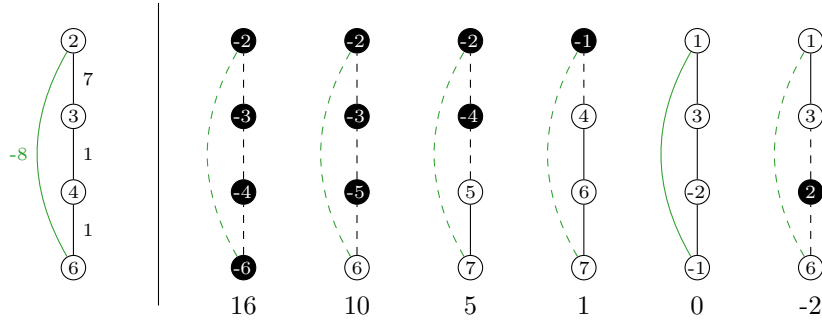


Figure 4: Depicted on the left is an instance of the multi-separator problem with respect to a graph, in black, and four interactions, including one non-edge, depicted in green. Depicted next to this graph, from left to right, are the iterations of the greedy algorithm defined in Section 4. In each iteration, the separator consists of the nodes that are depicted as solid black circles. Initially, all nodes are in the separator. Separated interactions are depicted as dashed lines. The number inside each node is the potential of that node in the respective iteration. Written below each graph is the current total cost. It can be seen in this example that the cost decreases with increasing iteration, until all nodes have a non-negative potential.

problem are not designed for the instances constructed in the proof of Theorem 1. For example, greedy additive edge contraction starting from singleton components (Keuper et al., 2015) results in the feasible solution in which every node v is put together with its copy \bar{v} , and *all* nodes v, w with $\{v, w\} \in E$ remain in distinct components.

Here, we pursue a different approach and define local search algorithms for the multi-separator problem specifically. As local transformations, we consider the insertion and removal of single nodes into and from the separator. We perform these transformations greedily, always considering one that decreases the cost function maximally: For any separator $S \subseteq V$ and any node $v \in V \setminus S$ not in the separator, we let $d(S, v)$ denote the difference in cost that results from the insertion of v into the separator S , i.e.

$$d(S, v) = \left(\sum_{u \in S \cup \{v\}} c_u + \sum_{f \in F(S \cup \{v\})} c_f \right) - \left(\sum_{u \in S} c_u + \sum_{f \in F(S)} c_f \right) = c_v + \sum_{f \in F(S \cup \{v\}) \setminus F(S)} c_f. \quad (4)$$

Here, $F(S \cup \{v\}) \setminus F(S)$ is the set of interactions that are separated by $S \cup \{v\}$ but not by S . In other words, it is the set of interactions not separated by S for which v is a cut-node in the graph obtained by removing the nodes in S from G . With this, we define the *greedy potential* function as

$$p(S, v) = \begin{cases} d(S, v) & \text{if } v \notin S \\ -d(S \setminus \{v\}, v) & \text{if } v \in S \end{cases}.$$

This function assigns to each node $v \in V$ the difference in cost that results from inserting v into the separator S , if $v \notin S$, or removing v from the separator S , if $v \in S$. With this potential function, we specify a local search algorithm as follows: Starting from an initial separator $S \subseteq V$, e.g. $S = V$ or $S = \emptyset$, we enter an infinite loop. Firstly, we choose a node $v \in \operatorname{argmin}_{u \in V} p(S, u)$ with the most negative potential. Then, if $p(S, v) \geq 0$, we terminate. If $p(S, v) < 0$, we distinguish two cases: If $v \in S$, we remove v from the separator, i.e. $S \leftarrow S \setminus \{v\}$. If $v \notin S$, we insert v into the separator, i.e. $S \leftarrow S \cup \{v\}$. As the total cost decreases strictly with increasing iteration, the algorithm terminates. An example is depicted in Figure 4.

Algorithms according to this specification need not be practical. In each iteration, the potentials of all nodes might be computed in order to identify a node with the most negative potential. Below, we define practical algorithms which are restricted to only one type of local transformation: removal of a single node from the separator, in Section 4.1, and insertion of a single node into the separator, in Section 4.2. In fact, we treat these cases symmetrically. This is possible for the multi-separator problem, thanks to Theorem 8, and would not be possible for the lifted multicut-problem, due to Theorem 9.

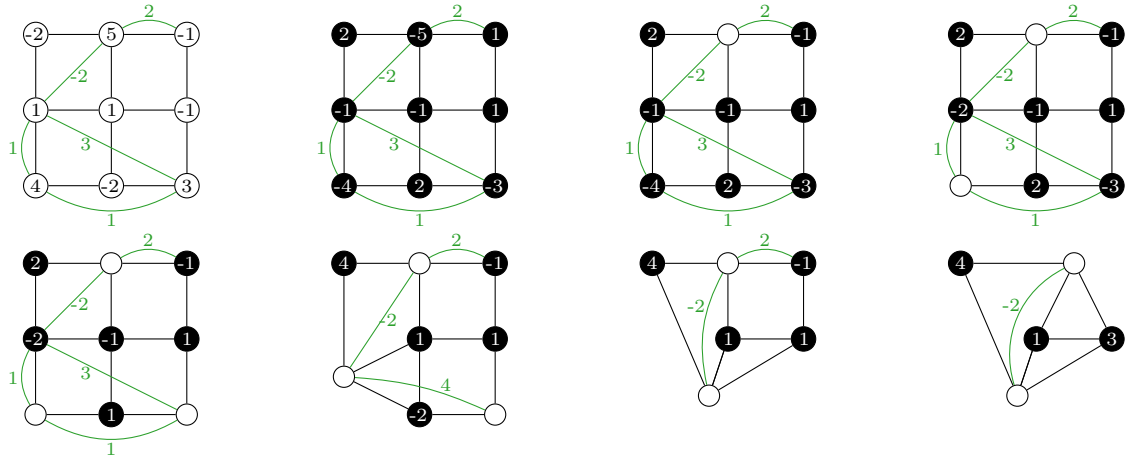


Figure 5: Depicted on the top left is an instance of the multi-separator problem consisting of a graph (black) and a set of interactions (green). Each node and every interaction has a cost. The second graph on the top depicts the initial feasible solution of Algorithm 1, i.e. all nodes are in the separator, and the potential of each node is precisely the negative of its cost. The subsequent graphs illustrate the iterations of Algorithm 1. In each iteration, one node is removed from the separator, all neighboring nodes that are not in the separator are contracted, and the potentials of all nodes in the separator are updated. The algorithm terminates after six iterations, as all nodes in the separator have a non-negative potential.

4.1 Greedy Separator Shrinking

In this section, we discuss Algorithm 1, a local search algorithm we call *greedy separator shrinking* (GSS) that starts with the separator $S = V$ containing all nodes and, in every iteration, removes from the separator one node so as to reduce the cost maximally. The operations of this algorithm are shown for one example in Figure 5.

The algorithm maintains two graphs, (V^t, E^t) and (V^t, F^t) with edge costs $c^t : F^t \rightarrow \mathbb{R}$, a separator S^t , and a function $p^t : S^t \rightarrow \mathbb{R}$. Initially, $S^0 = V^0 = V$ and $E^0 = E$ and $F^0 = F$ and $p_v^0 = -c_v$ for all $v \in V$. In every iteration t , the set V^t contains all nodes in the separator S^t and, in addition, all components of the subgraph of (V, E) induced by $V \setminus S^t$. When a node v is removed from the separator (Line 8) the subsequent graphs (V^{t+1}, E^{t+1}) and (V^{t+1}, F^{t+1}) are obtained by contracting in (V^t, E^t) and (V^t, F^t) the set containing v and all neighbors of v that are not elements of the separator into a new node v' (Line 9 to Line 13). The contraction may result in parallel edges which are merged into one edge (Line 12). Analogously, parallel interactions are merged into one interaction whose costs is the sum of the costs of the merged interactions (Line 13 to Line 18). Subsequently, the potentials of the nodes in S^{t+1} are computed with respect to the contracted graphs (V^{t+1}, E^{t+1}) , (V^{t+1}, F^{t+1}) , and c^{t-1} (Line 19 to Line 24). By definition of the potential in (4), the potentials of all nodes that are not adjacent to the new component remain unchanged (Line 24). The potentials of the nodes adjacent to v' are recomputed according to (4) (Line 22).

Let us compare greedy separator shrinking (GSS) for the multi-separator problem to greedy additive edge contraction (GAEC) as defined by Keuper et al. (2015) for the (lifted) multicut problem: In each iteration of GSS, one node is removed from the separator and thus, an unconstrained number of components become connected to form one component. In each iteration of GAEC, one edge is contracted and thus, precisely two components are joined to become one component. Moreover, GSS removes the node with the most negative potential, while GAEC contracts the edge with the largest positive cost. In GSS, the computation of the node potentials of the graph obtained by removing one node from the separator requires the operations in Line 19 to Line 24 that are illustrated also in Figure 6. In GAEC, the computation of the edge costs of the graph obtained by contracting an edge consists in simply summing the costs of parallel edges.

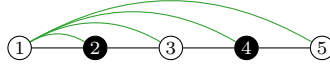


Figure 6: Depicted above are a graph (in black) and a set of interactions (in green). Let $S^t = \{2, 4\}$ be the separator at iteration t of the GSS algorithm. The current potential of Node 2 is $p_2^t = -c_2 - c_{\{1,2\}} - c_{\{1,3\}}$. If Node 4 is removed from the separator in iteration t , the potential of Node 2 becomes $p_2^{t+1} = -c_2 - c_{\{1,2\}} - c_{\{1,3\}} - c_{\{1,4\}} - c_{\{1,5\}}$.

Lemma 2. *Algorithm 1 has a worst case time complexity of $\mathcal{O}(|V|^2 \log |V| d^2)$ where d is the degree of the input graph $G = (V, E)$.*

Proof. For $v \in V$, let $\deg_{(V,E)}(v)$ be the degree of v in the graph (V, E) . Let $d = \max_{v \in V} \deg_{(V,E)}(v)$ be the degree of the graph (V, E) . Observe for all t and all $v \in S^t$ that $\deg_{(V^t, E^t)}(v) \leq \deg_{(V,E)}(v)$ because the contractions that lead to the graph (V^t, E^t) only involve nodes in $V^t \setminus S^t$. In contrast, the degree of the nodes in $V^t \setminus S^t$ is not bounded in such a way; in fact, it is in $\mathcal{O}(n)$. The same observation holds true for the interaction graphs (V, F) and (V^t, F^t) .

The algorithm terminates after at most $|V|$ iterations. The runtime of each iteration is dominated by the time for recomputing the potentials of the nodes that are adjacent to the newly formed component (Line 22). By the above observation, the number of nodes for which the potential needs to be recomputed is $\mathcal{O}(|V|)$. Furthermore, the degree of each node $u \in S^{t+1}$ is bounded by d . Therefore, the size of the set N (Line 21) that contains u and the neighbors of u in (V^{t+1}, E^{t+1}) that are not in the separator is bounded by $d + 1$. To compute the potential in Line 22, all interactions between any two nodes in N need to be identified. As the set N contains nodes that are not in the separator, the degree of these nodes is not bounded by d but is instead in $\mathcal{O}(n)$. For each of the nodes $w \in N$, it needs to be checked if any of the other nodes $w' \in N \setminus \{w\}$ is adjacent to w in the interaction graph (V^{t+1}, F^{t+1}) . By maintaining for each node a reference to all its neighbors in the interaction graph in a sorted array, this can be checked in time $\mathcal{O}(\log |V|)$. Consequently, all interactions in $\{f \in F^{t+1} \mid f \subseteq N\}$ can be identified in time $\mathcal{O}(d^2 \log |V|)$. \square

The C++ implementation of Algorithm 1 in the supplement utilizes a priority queue of all nodes in the separator where the node with the smallest potential has the highest priority. In order to process updates of priorities (increases and decreases), we store a version number for each node and define as entries of the priority queue pairs consisting of a node and a version number. Initially, the version numbers of all nodes are zero. Whenever the priority of a node changes, we increment the version number associated with that node and insert into the priority queue an additional element consisting of that node and the updated version number. This facilitates updates of the potential of a node in constant time in Line 22. Whenever we pop the highest-priority node from the queue (Line 5), we check whether its version number is the highest ever associated with that node. If so, we process the node. Otherwise, we discard that entry and pop the next. This implementation does not improve over the worst case time complexity of Lemma 3. Measurements of the absolute runtime for specific instances are reported in Figure 13, Section 5.

4.2 Greedy Separator Growing

In this section, we discuss Algorithm 2, a local search algorithm we call *greedy separator growing* (GSG) that starts with the separator $S = \emptyset$ being empty and, in every iteration, adds to the separator one node so as to reduce the cost maximally. The operations of this algorithm are shown for one example in Figure 7.

Before describing the algorithm in detail, we discuss one property informally: By adding a node to the separator S , other nodes that are not in the separator can become cut-nodes of the graph induced by $V \setminus S$. According to (4), the potential of a node $v \notin S$ is the cost of the node c_v plus the costs of all interactions that are separated by $S \cup \{v\}$ and not by S . If v is not a cut-node, then the set of interactions that are separated by $S \cup \{v\}$ but not by S is a subset of the interactions that

Algorithm 1: Greedy Component Shrinking (GSS)

Data: Graph $G = (V, E)$, interactions $F \subseteq \binom{V}{2}$, costs $c : V \cup F \rightarrow \mathbb{R}$
Result: separator $S \subseteq V$

- 1 $V^0 := V, E^0 := E, F^0 := F, c^0 := c, S^0 := V$
- 2 $p_v^0 := -c_v \forall v \in V^0$
- 3 $t := 0$
- 4 **while** $S^t \neq \emptyset$ **do**
- 5 $v \in \operatorname{argmin}_{s \in S^t} p_s^t$
- 6 **if** $p_v^t > 0$ **then**
- 7 **break**
- 8 $S^{t+1} := S^t \setminus \{v\}$
- 9 $C := \{v\} \cup \{u \in V^t \mid \{u, v\} \in E^t \text{ and } u \notin S\}$
- 10 create new node v'
- 11 $V^{t+1} := V^t \setminus C \cup \{v'\}$
- 12 $E^{t+1} := E^t \setminus \{\{u, w\} \in E^t \mid u \in C \text{ or } w \in C\} \cup \{\{v', u\} \mid \exists w \in C : \{u, w\} \in E^t\}$
- 13 $F^{t+1} := F^t \setminus \{\{u, w\} \in F^t \mid u \in C \text{ or } w \in C\} \cup \{\{v', u\} \mid \exists w \in C : \{u, w\} \in F^t\}$
- 14 **for** $\{u, w\} \in F^{t+1}$ **do**
- 15 **if** $v' \notin \{u, w\}$ **then**
- 16 $c_{\{u, w\}}^{t+1} := c_{\{u, w\}}^t$
- 17 **else**
- 18 $c_{\{v', w\}}^{t+1} := \sum_{u \in C : \{u, w\} \in F^t} c_{\{u, w\}}^t$
- 19 **for** $u \in S^{t+1}$ **do**
- 20 **if** $\{v', u\} \in E^{t+1}$ **then**
- 21 $N := \{u\} \cup \{w \in V^{t+1} \setminus S^{t+1} \mid \{u, w\} \in E^{t+1}\}$
- 22 $p_u^{t+1} := -c_u - \sum_{f \in F^{t+1}, f \subseteq N} c_f$
- 23 **else**
- 24 $p_u^{t+1} := p_u^t$
- 25 $t := t + 1$
- 26 **return** S^t

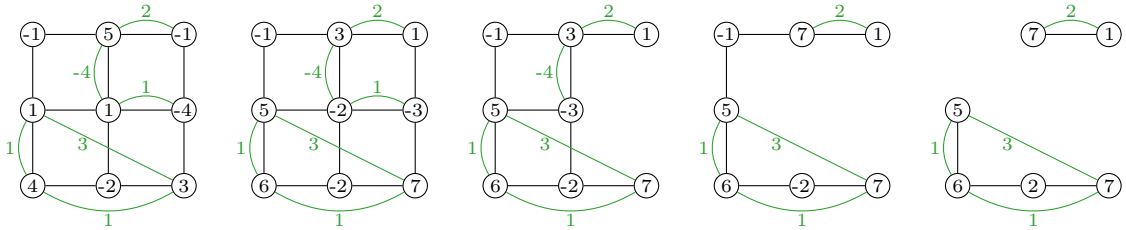


Figure 7: Depicted on the left is an instance of the multi-separator problem consisting of a graph (black) and a set of interactions (green). Each node and every interaction has a costs. The second graph depicts the starting solution of Algorithm 2, i.e. no nodes are in the separator, and all nodes form one large component. The potential of each node is the cost of that node plus the sum of the costs of all interactions adjacent to that node. The subsequent graphs illustrate the iterations of Algorithm 2. In each iteration, a node with minimal negative potential is added to the separator, i.e. deleted from the graph, and the potentials of the remaining nodes are updated. The algorithm terminates after the three iterations, as all remaining nodes have non-negative potential. In the last iteration, the node in the bottom center has the most negative potential of -2 . However, it is a cut-node and would separate the two interactions adjacent to the bottom right node. Therefore, its potential is updated to $2 = -2 + 1 + 3$. Now, the node with the most negative potential is the top left node, which is deleted from the graph.

are adjacent to v . However, if v is a cut-node, then the set of interactions that are separated by $S \cup \{v\}$ but not by S can contain additional interactions that are not adjacent to v . As identifying cut-nodes and those interactions that would be separated by adding a cut-node to the separator is computationally expensive (Hopcroft and Tarjan, 1973), the GSG algorithm checks if a node is a cut-node only before this node is added to the separator. If it is a cut-node, then the potential of that node is recomputed by identifying all interactions that would be separated if the node was added to the separator. By this strategy, the true potential of a node can be smaller than the potential that is known to the algorithm. As a result, a node v can be added to the separator even though there exists another node u whose potential is strictly less than that of v , but the true potential of u is not known to the algorithm. Yet, in the special case where the costs of all interactions that are not edges in G , have non-negative cost, the true potential of a node cannot be smaller than the potential that is known to the algorithm. Therefore, in that special case, the algorithm always adds to the separator one node that reduces the cost maximally.

More specifically, GSG works as described below and as illustrated for one example in Figure 7. The algorithm maintains an induced subgraph (V^t, E^t) of the input graph (V, E) , a subset of interactions $F^t \subseteq F$, a function $p^t : V^t \rightarrow \mathbb{R}$, and a map $\text{CN}^t : F^t \rightarrow 2^{V^t}$ from each $f \in F^t$ to the subset of nodes in V^t that are identified as f -cut-nodes in (V^t, E^t) . Initially, $V^0 = V$, $E^0 = E$, $F^0 = F$, $p_v^0 := c_v + \sum_{\{u,v\} \in F} c_{\{u,v\}}$ for all $v \in V$, and $\text{CN}_{\{u,v\}}^0 = \{u,v\}$ for all $\{u,v\} \in F^0$. In every iteration t , the set V^t contains all nodes that are not in the separator, the set E^t contains the edges of the subgraph of (V, E) induced by V^t , and the set F^t contains all interactions that are not separated by $V \setminus V^t$ in (V, E) . Note that the potential p_v^0 as computed in Line 2 does not account for the interactions that are not adjacent to v , for which v is a cut-node. Also, the set CN_f^0 only accounts for the cut-nodes of f that are adjacent to f . Once a node is selected to be added to the separator, i.e. deleted from V^t (Line 6), the potential of that node is recomputed according to (4) (Line 9). For the separator $S = V \setminus V^t$, we have $F(S \cup \{v\}) \setminus F(S) = F^t(\{v\})$, i.e. the set of interactions in F that are separated by $S \cup \{v\}$ but not by S in (V, E) is equal to the set of interactions in F^t that are separated by $\{v\}$ in (V^t, E^t) . The set $F^t(\{v\})$ is computed by first computing the components of the subgraph of (V^t, E^t) induced by $V^t \setminus \{v\}$ and then selecting all interactions in F^t whose endpoints lie in distinct components. This takes linear time. For all interactions $f \in F^t(\{v\})$, the node v is added to the set CN_f^t of nodes that have been identified as f -cut-nodes in (V^t, E^t) (Line 11). If the recomputed potential of v is positive, or if v is no longer the node with the smallest potential, a new node with smallest potential is selected (Line 13). Otherwise, the node v is added to the separator, i.e. deleted from the graph (Line 14 to Line 16). All interactions $F^t(\{v\})$ that are separated by deleting v from the graph can no longer be separated by deleting any other node from the graph. The potentials of all nodes that have been identified as cut-nodes for any of the interactions in $F^t(\{v\})$ are updated accordingly (Line 17 to Line 20). For all interactions $f \in F^{t+1}$, the nodes that have been identified as f -cut-nodes remain unchanged (Line 22).

Remark 3. Algorithm 2 exploits the fact that the node variables in the multi-separator problem (MSP) are unconstrained, i.e. any node subset $S \subseteq V$ is a feasible solution. This is in contrast to the lifted multicut problem (LMP) where not all edge subsets $M \subseteq E$ are feasible. Thus, an analog to Algorithm 2 for (LMP) that iteratively adds single edges to a set of cut edges is not guaranteed to output a feasible solution to (LMP).

Remark 4. Algorithm 2 can be applied to arbitrary instances of (MSP), including those where not all costs of interactions $F \setminus E$ are non-negative. For those, however, it is not guaranteed that, in each iteration, the node added to the separator decreases the cost maximally.

Lemma 3. *Algorithm 2 has a worst case time complexity of $\mathcal{O}(|V|^2(|V| + |E| + |F|))$.*

Proof. There are at most $|V|$ iterations in which a node is removed from the graph, i.e. added to the separator (Line 14), since each node can be removed at most once. However, there can be more than $|V|$ iterations as a node v might be discarded for removal from the graph (Line 13) if the potential of that node is, after recomputing it in Line 9, no longer minimal. In the worst

Algorithm 2: Greedy Separator Growing (GSG)

Data: Connected graph $G = (V, E)$, interactions $F \subseteq \binom{V}{2}$, costs $c : V \cup F \rightarrow \mathbb{R}$ with $c_f \geq 0$ for $f \in F \setminus E$

Result: separator $S \subseteq V$

```
1  $V^0 := V, E^0 := E, F^0 := F$ 
2  $p_v^0 := c_v + \sum_{\{u,v\} \in F} c_{\{u,v\}} \forall v \in V^0$ 
3  $CN_{\{u,v\}}^0 := \{u, v\} \forall \{u, v\} \in F^0$ 
4  $t := 0$ 
5 while  $V^t \neq \emptyset$  do
6    $v \in \operatorname{argmin}_{u \in V^t} p_u^t$ 
7   if  $p_v^t > 0$  then
8     break
9    $p_v^t := c_v + \sum_{f \in F^t(\{v\})} c_f$ 
10  for  $f \in F^t(\{v\})$  do
11     $CN_f^t := CN_f^t \cup \{v\}$ 
12  if  $p_v^t > 0$  or  $p_v^t > \min_{u \in V^t} p_u^t$  then
13    continue
14   $V^{t+1} := V^t \setminus \{v\}$ 
15   $E^{t+1} := E^t \setminus \{e \in E \mid v \in E\}$ 
16   $F^{t+1} := F^t \setminus F^t(\{v\})$ 
17   $p^{t+1} := p^t$ 
18  for  $f \in F^t(\{v\})$  do
19    for  $u \in CN_f^t$  do
20       $p_u^{t+1} := p_u^{t+1} - c_f$ 
21  for  $f \in F^{t+1}$  do
22     $CN_f^{t+1} := CN_f^t$ 
23   $t := t + 1$ 
24 return  $V \setminus V^t$ 
```

case, all nodes in V^t are discarded once, without removing a node from the graph. After that, the potentials p_v^t of all nodes $v \in V^t$ are correct. Subsequently, the recomputation of the potential in Line 9 will not change the potential, and thus, this node will not be discarded. Overall, there are $\mathcal{O}(|V|^2)$ iterations in which Lines 6 to 13 are executed.

The set of interactions $F^t(\{v\})$ that are separated by $\{v\}$ in (V^t, E^t) can be identified by, firstly, computing the components of the subgraph of (V^t, E^t) that is induced by $V^t \setminus \{v\}$ and, secondly, selecting all interactions in F^t whose endpoints belong to different components. This can be done in time $\mathcal{O}(|V| + |E| + |F|)$, using breadth-first search for computing the components. Therefore, Lines 6 to 17 can be executed in time $\mathcal{O}(|V| + |E| + |F|)$. Clearly, Lines 18 to 20 can be executed in time $\mathcal{O}(|V||F|)$. By the previous argument, these lines are executed at most $|V|$ times. Thus follows the claim. \square

As for Algorithm 1, the C++ implementation of Algorithm 2 in the supplementary material of this article utilizes a priority queue for efficiently querying a node with smallest potential. Also this implementation does not improve over the worst case time complexity of Lemma 3. Measurements of the absolute runtime for specific instances are reported in Figure 13, Section 5.

5 Application to image segmentation

5.1 Volume images of simulated foams and filaments

In order to examine the multi-separator problem defined in Section 3, in connection with the algorithms introduced in Section 4, empirically, in a well-defined and adjustable setting, we synthesize two types of volume images, volume images of filaments (Figure 8), and volume images

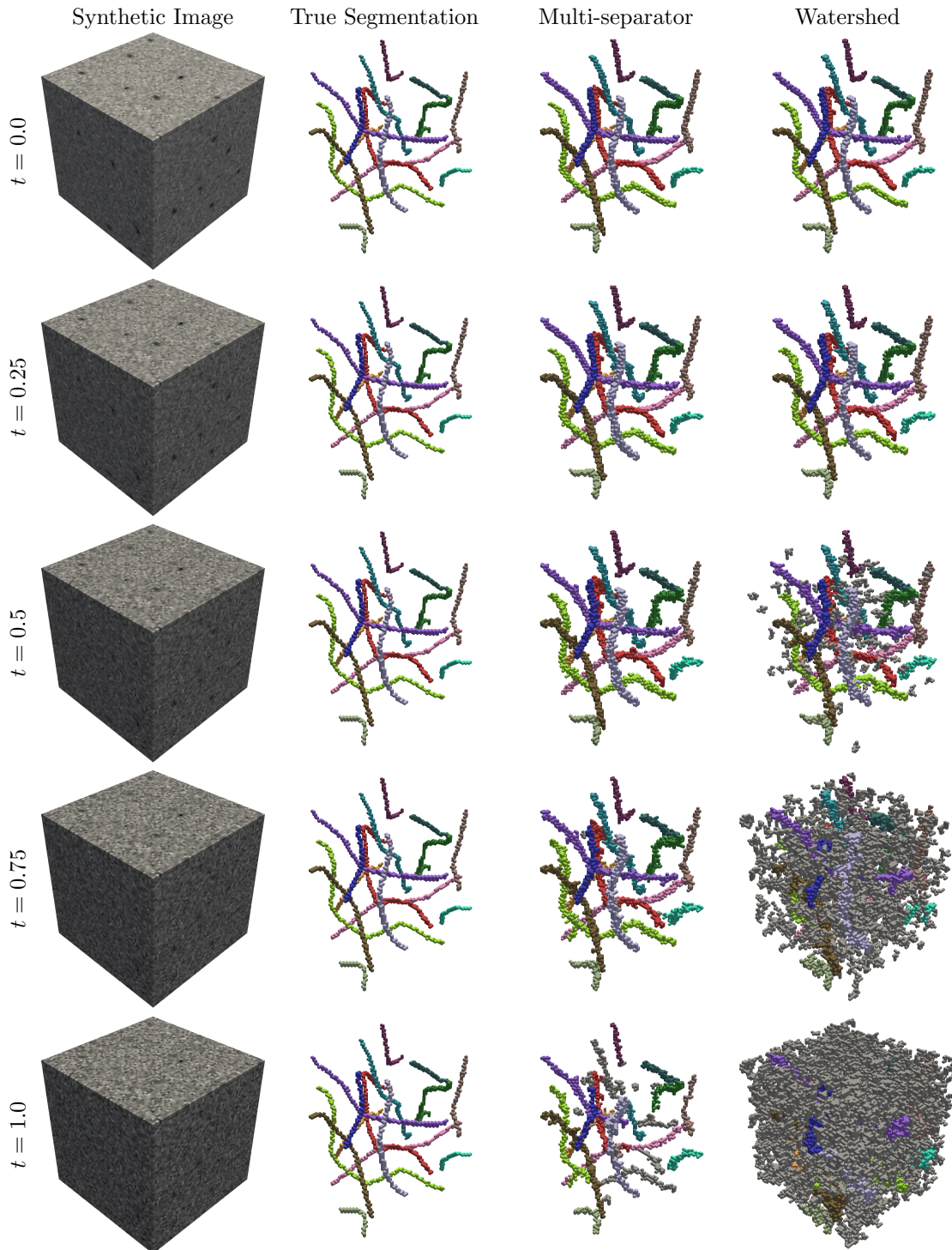


Figure 8: Depicted above are multi-separators of volume images of simulated **filaments** with five amounts of noise, t (rows): The true multi-separator (Column 2), the multi-separators output by Algorithm 2 (Column 3), and the multi-separator output by the watershed algorithm (Column 4). For each t , the parameters (θ_{start} and θ_{end} for the watershed algorithm, b for Algorithm 2) are chosen so as to minimize the average VI-WS across those images of the data set with the amount of noise t . Components that do not match with any true component are depicted in gray. For clarity, only components containing at least 10 voxels are shown.

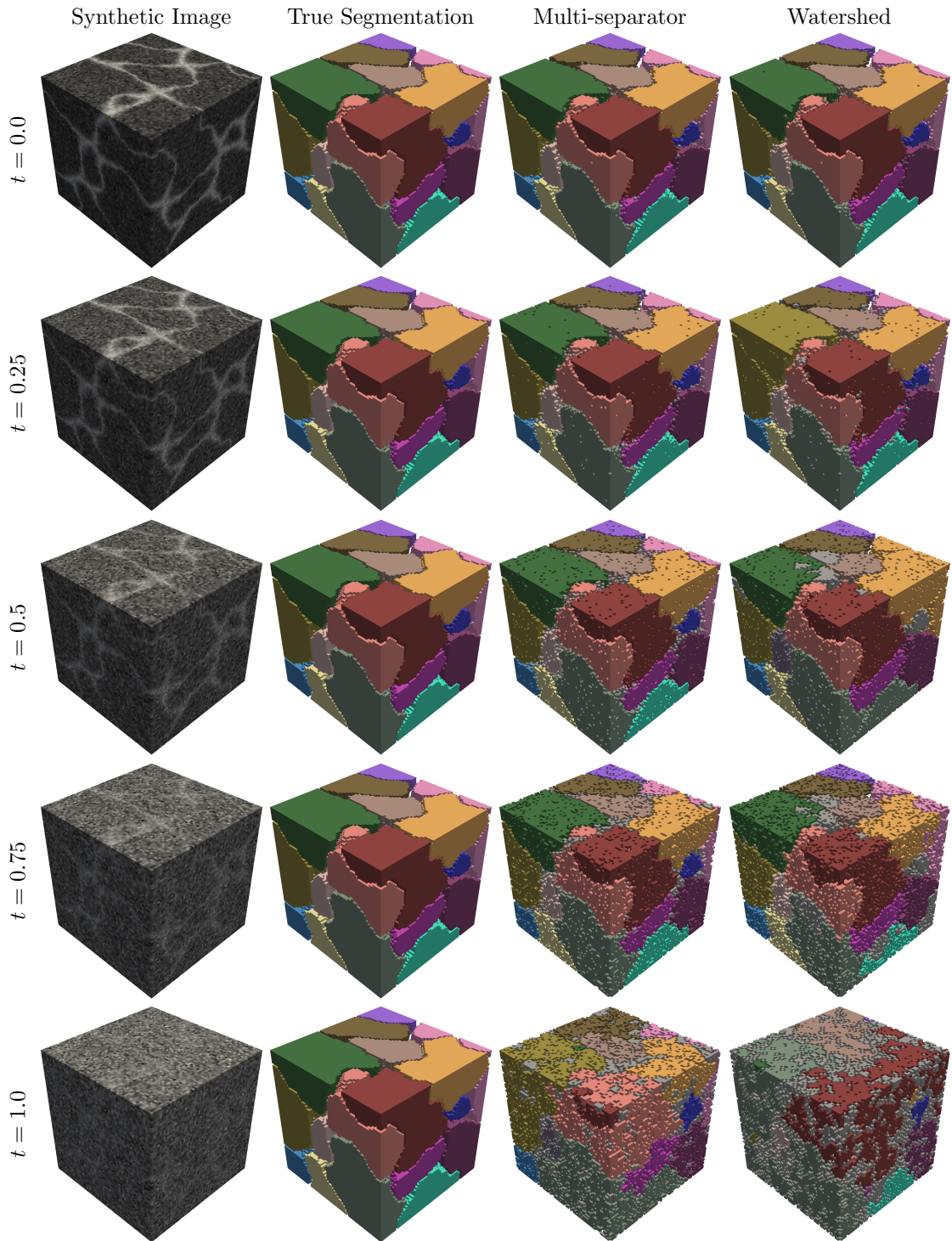


Figure 9: Depicted above are multi-separators of volume images of simulated **foam cells** with five amounts of noise, t (rows): The true multi-separator (Column 2), the multi-separator output by Algorithm 1 (Column 3), and the multi-separator output by the watershed algorithm (Column 4). For each t , the parameters (θ_{start} and θ_{end} for the watershed algorithm, b for Algorithm 1) are chosen so as to minimize the average VI-WS across those images of the data set with the amount of noise t . Components that do not match with any true component are depicted in gray.

of foam cells (Figure 9). Both types of volume images are constructed in two steps. The first step is to construct a binary volume image of $m \times m \times m$ voxels in which voxels labeled 0 depict randomly constructed filaments or foam cells, and voxels labeled 1 depict void or foam membranes separating these structures. The second step is to construct from these binary volume images and a parameter $t \in [0, 1]$ defining an amount of noise, gray scale volume images of the same size. We repeat the first step in order to obtain volume images of different filaments or foam cells. We repeat the second step in order to obtain volume images with different amounts of noise. The procedure is described in detail in Appendix A.1. Overall, we synthesize 10 volume images of filaments and 10 volume images of foam cells, each with 21 different amounts of noise, $t = \frac{i}{20}$ for $i = 0, \dots, 20$. This defines a data set of 20 binary volume images and 420 gray scale volume images. Examples are depicted in Figures 8 and 9.

The task posed by this data consists in reconstructing the binary volume image, henceforth also referred to as the *truth*, from the associated gray scale volume image. As with many synthetic data sets, this task is not necessarily difficult to solve if one exploits the complete knowledge of how the data is constructed. We use it here to pose non-trivial problems by artificially ignoring much of this knowledge.

5.2 Problem setup

We state the task of reconstructing the true binary volume image from a gray scale volume image in the form of the multi-separator problem (MSP). To this end, we consider the grid graph consisting of one node for each voxel and edges connecting precisely the adjacent voxels. For volume images of filaments, we consider as interactions the edges of the voxel grid graph as well as those pairs of voxels that have a rounded Euclidean distance of 8 and a positive cost (defined below). For volume images of foam cells, we define the set of interactions by a collection of offsets in the three directions of the voxel grid graph, namely $\mathcal{O} = \{(1, 0, 0), (0, 1, 0), (0, 0, 1), (5, 0, 0), (0, 5, 0), (0, 0, 5), (0, 4, 4), (0, 4, -4), (4, 4, 0), (4, -4, 0), (4, 0, 4), (4, 0, -4), (3, 3, 3), (3, 3, -3), (3, -3, 3), (3, -3, -3)\}$. For any voxel v at coordinates (x, y, z) and any $(\delta_x, \delta_y, \delta_z) \in \mathcal{O}$, the voxel v is connected by an interaction to the voxel at coordinates $(x + \delta_x, y + \delta_y, z + \delta_z)$ if these coordinates are within the bounds of the grid.

For a voxel v with gray value $g \in (0, 1)$, we define the node cost as $c_v = \log\left(\frac{1-g}{g}\right)$.

For an interaction $\{u, v\}$ between two voxels u and v , we define the interaction cost $c_{\{u, v\}}$ with respect to the costs of the voxels that lie on the digital straight line connecting u and v in the volume image. For volume images of filaments, we define $c_{\{u, v\}}$ as the median of the costs of the voxels on that line. Thus, if at least one half of the voxels on the line have positive cost (i.e. likely belong to a filament), then the interaction $\{u, v\}$ is attractive. Otherwise, it is repulsive. For volume images of foam cells, we define $c_{\{u, v\}}$ as the minimum of the costs of the voxels on that line. Thus, if there exists a voxel on the line that has negative cost (i.e. likely belongs to a membrane), then the interaction $\{u, v\}$ is repulsive. Otherwise, it is attractive.

The instances of the multi-separator problem thus constructed are artificial in several ways: Firstly, we define the node costs with respect to the gray value of just one voxel, whereas most researchers working with real data, including Lee et al. (2021), consider such costs to depend on the gray values of voxel neighborhoods and estimate (learn) these dependencies from examples (Minaee et al., 2022). Secondly, the node cost c_v of a voxel v labeled 1 in the true binary image, will, in expectation, be negative, while the cost c_v of a voxel v labeled 0 in the true binary image, will, in expectation, be positive. This unbiasedness of the node costs holds by construction of the volume images, more specifically, because the average of the mean gray value of filaments and foam cells, on the one hand, and the mean gray value of void and foam membranes, on the other hand, is exactly $\frac{1}{2}$ (Section 5.1 and Appendix A.1). We exploit this knowledge in the problem statement. However, we do not limit our analysis to unbiased instances of the multi-separator problem. Instead, we add an bias systematically, as described in Section 5.5 below.

5.3 Alternative

In order to compare the output of the algorithms we define in Section 4 to the output of an algorithm that is well-understood and widely-used, we compute multi-separators from each volume image also by means of a watershed algorithm (cf. Roerdink and Meijster, 2000, for an overview), more specifically, the watershed algorithm and implementation by van der Walt et al. (2014). Therefor, we introduce two parameters, $\theta_{\text{start}}, \theta_{\text{end}} \in [0, 1]$ with $\theta_{\text{start}} \leq \theta_{\text{end}}$. θ_{start} defines seeds for the watershed algorithm as the maximal connected components of all voxels with gray value less than θ_{start} . θ_{end} defines the gray value at which the flood-filling procedure of the watershed algorithm is terminated. We consider several combinations of these parameters, from intervals large enough to be clearly sub-optimal at the end-points, for all amounts of noise. For filaments, we consider 41 values of θ_{start} equally spaced in $[0.45, 0.65]$, and 41 values of θ_{end} equally spaced in $[0.5, 0.7]$. For foam cells, we consider 51 values of θ_{start} equally spaced in $[0.0, 0.5]$, and 21 values of θ_{end} equally spaced in $[0.4, 0.6]$. The effect of the parameters θ_{start} and θ_{end} is depicted in Appendix A.3.

5.4 Metric

In order to measure a distance between any multi-separator computed from a gray scale volume image, on the one hand, and the true multi-separator, i.e. the set of voxels labeled 1 in the true binary volume image, on the other hand, we take two steps. Firstly, we consider partitions of the node set induced by these two separators. Secondly, we measure the distance between these partitions by evaluating a metric known as the variation of information (Arabie and Boorman, 1973; Meilă, 2007). The two steps are described in more detail below.

For any multi-separator S of a graph $G = (V, E)$, we consider the partition of the node set V consisting of (i) the inclusion-wise maximal subsets of $V \setminus S$ that induce a component of the subgraph of G induced by $V \setminus S$, and (ii) one singleton set $\{v\}$ for every node $v \in S$.

For any two partitions \mathcal{A}, \mathcal{B} of V , any probability mass function $p: V \rightarrow [0, 1]$ and the extension of p to subsets of V such that for any $U \subseteq V$, we have $p(U) = \sum_{v \in U} p(v)$, the variation of information holds

$$\begin{aligned} \text{VI}_p(\mathcal{A}, \mathcal{B}) &= 2H_p(\mathcal{A}, \mathcal{B}) - H_p(\mathcal{A}) - H_p(\mathcal{B}) \\ &= H_p(\mathcal{A} \mid \mathcal{B}) + H_p(\mathcal{B} \mid \mathcal{A}) \end{aligned}$$

with

$$\begin{aligned} H_p(\mathcal{A}) &= - \sum_{A \in \mathcal{A}} p(A) \log_2 p(A) \\ H_p(\mathcal{A}, \mathcal{B}) &= - \sum_{A \in \mathcal{A}, B \in \mathcal{B}, A \cap B \neq \emptyset} p(A \cap B) \log_2 p(A \cap B) \\ H_p(\mathcal{A} \mid \mathcal{B}) &= H_p(\mathcal{A}, \mathcal{B}) - H_p(\mathcal{B}) \end{aligned}$$

the entropy, joint entropy and conditional entropy with respect to the probability mass function p .

Usually, one considers the variation of information with respect to the uniform probability mass $p(v) = |V|^{-1}$ for all $v \in V$ (Arabie and Boorman, 1973; Meilă, 2007). In our experiments, there is an imbalance between the number of voxels in the true separator T and the number of voxels in the complement $V \setminus T$. For filaments, most voxels are in T . For foam cells, most voxels are in $V \setminus T$. We chose $p(v) = \frac{1}{2}|T|^{-1}$ for all $v \in T$ and $p(v) = \frac{1}{2}|V \setminus T|^{-1}$ for all $v \in V \setminus T$. This way, nodes in the separator and nodes not in the separator both contribute $\frac{1}{2}$ to the total probability mass. We refer to the metric thus obtained as the *variation of information between separator-induced weighted partitions with singletons* and abbreviate it as VI-WS. The conditional entropies $H_p(\mathcal{A} \mid \mathcal{B})$ and $H_p(\mathcal{B} \mid \mathcal{A})$ are indicative of false cuts and false joins of \mathcal{A} compared to \mathcal{B} . We abbreviate these as FC and FJ.

Complementary to VI-WS, we report also the variation of information with respect to the uniform probability mass function and partitions of the set of those voxels that are neither in

the true multi-separator nor in the computed multi-separator. We refer to this metric as the *variation of information with respect to non-separator nodes*. We abbreviate this metric as VI-NS and abbreviate the conditional entropies due to false cuts and false joins as FC-NS and FJ-NS. The metric VI-NS suffers from a degeneracy: If the computed separator contains all nodes, VI-NS evaluates to zero. This degeneracy of VI-NS has been the motivation for us to introduce VI-WS.

5.5 Experiments

For each volume image from the data set described in Section 5.1, we construct several instances of the multi-separator problem according to Section 5.2, each with a different bias $b \in \mathbb{R}$ added to all coefficients in the cost function. A positive bias penalizes voxels being in the separator; a negative bias rewards voxels being in the separator. We consider several biases, from intervals large enough to be clearly sub-optimal at the end-points, for all amounts of noise (Figure 12). For both filaments and foam cells, we consider 51 values equally spaced in $[-0.25, 0.25]$. For each instance of the multi-separator problem thus obtained, we compute one multi-separator, using Algorithm 2, for filaments, and Algorithm 1, for foam cells.

For each volume image and every combination of the parameters $\theta_{\text{start}}, \theta_{\text{end}}$, we compute one additional multi-separator by means of the watershed algorithm described in Section 5.3.

We measure the distance between each multi-separator thus computed from a gray scale volume image, on the one hand, and the set of voxels labeled 1 in the true binary image, on the other hand, by evaluating the metric described in Section 5.4.

In addition, we measure the runtime of our single-thread C++ implementation of Algorithms 1 and 2 as a function of the size of a volume image, for additional volumes images of $m \times m \times m$ voxels, with $m \in \{20, \dots, 216\}$, synthesized as described in Section 5.1 and Appendix A.1, with noise $t = 0.5$. From these, we construct instances of the multi-separator problem as described in Section 5.2. We measure the runtime on a Lenovo X1 Carbon laptop equipped with an Intel Core i7-10510U CPU @ 1.80GHz processor and 16 GB LPDDR3 RAM.

The complete C++ code for reproducing these experiments is included as supplementary material.

5.6 Results

Depicted in Figures 10 to 12 is the inaccuracy, i.e. the distance from the truth, of multi-separators computed by Algorithm 2 (for filaments), by Algorithm 1 (for foam cells) and by the watershed algorithm (for both), for volume images with different amounts of noise t . Depicted in Figures 8 and 9 are qualitative examples.

Figures 10 and 11 show, for each amount of noise t , the distribution of distances across those volume images in the data set that exhibit this amount of noise. Here, the parameters (b , for Algorithms 1 and 2, θ_{start} and θ_{end} for the watershed algorithm) are chosen so as to minimize the average VI-WS across those images of the data set with the amount of noise t . It cannot be seen from Figures 10 and 11 how sensitive the VI-WS is to the choice of the bias parameter b . To this end, Figure 12 shows the inaccuracy of multi-separators computed by Algorithm 2 (for filaments) or Algorithm 1 (for foam cells) as a function of the bias b .

Finally, Figure 13 shows measurements of the runtime of our implementations of Algorithms 1 and 2 for instances of the multi-separator problem of varying size.

5.7 Observations

5.7.1 General observations

For volume images with little noise, $t \leq 0.1$, Algorithms 1 and 2 and the watershed algorithm output a multi-separator almost without false joins or false cuts, and those inaccuracies that do occur have a small effect on the variation of information (Figures 10 and 11). For $t > 0.1$, multi-separators output by Algorithms 1 and 2 can be significantly closer to the truth than those output by the watershed algorithm in terms of the distance VI-WS. For $t \leq 0.5$, the multi-separators output

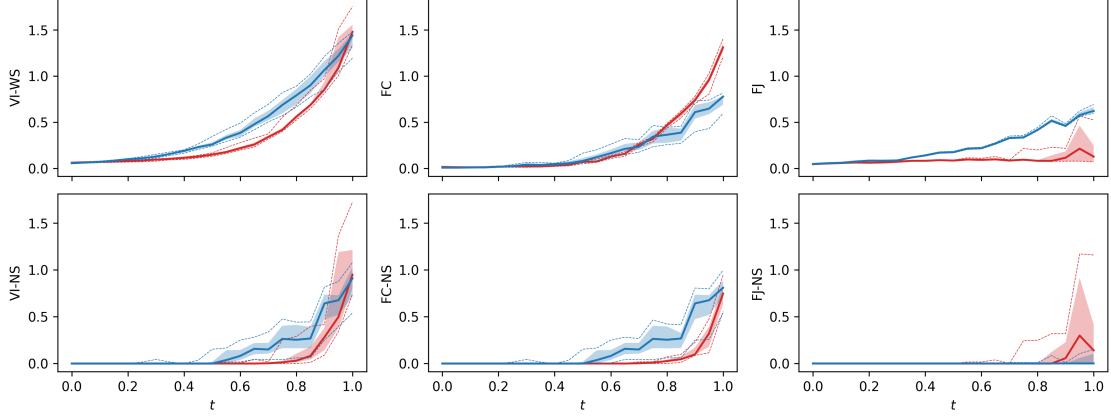


Figure 10: Depicted above is the inaccuracy (distance from the truth) of multi-separators computed by Algorithm 2 (red) or the watershed algorithm (blue), for volume images of **filaments** with different amounts of noise t . For each volume image, the parameters for both algorithms are chosen such that the multi-separator output by the algorithm minimizes the average VI-WS across those images of the data set with the amount of noise t . Depicted on top from left to right are the VI-WS as well as the conditional entropies due to false cuts (FC) and false joins (FJ). Depicted on the bottom from left to right are the variation of information with respect to only those voxels that are not labeled as separator in both the true multi-separator and the computed multi-separator (VI-NS) as well as the respective conditional entropies due to false cuts (FC-NS) and false joins (FJ-NS). Thick lines indicate the median across those images of the data set with the amount of noise t . Shaded areas indicate the second and third quartile. Dashed lines indicate the 0.1 and 0.9-quantile.

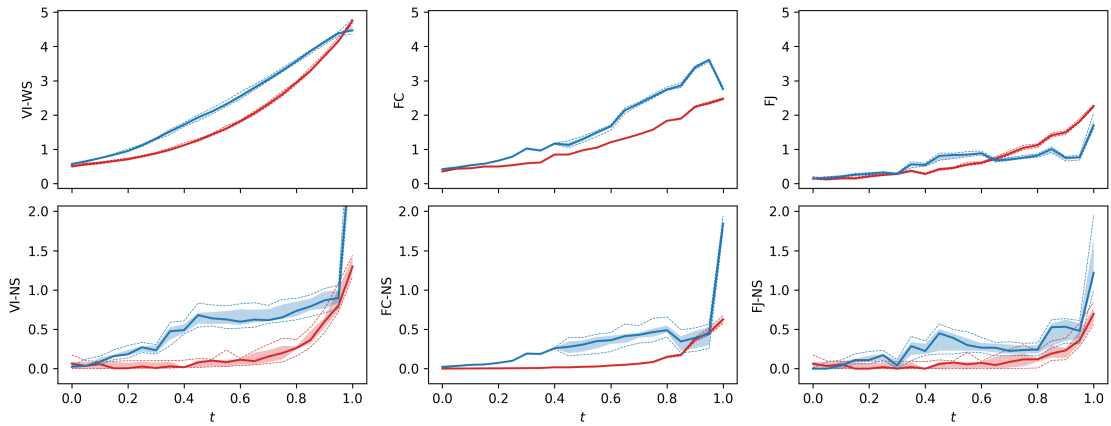


Figure 11: Depicted above is the inaccuracy (distance from the truth) of multi-separators computed by Algorithm 2 (red) or the watershed algorithm (blue), for volume images of **foam cells** with different amounts of noise t . The interpretation of the figure is completely analogous to Figure 10.

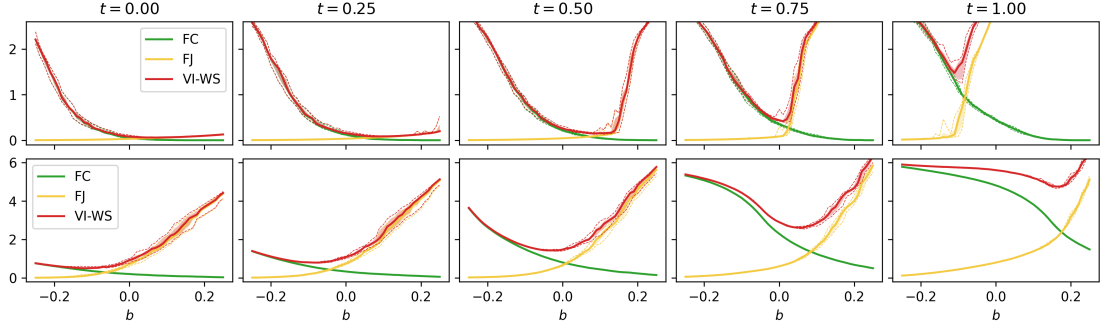


Figure 12: Depicted above is the inaccuracy (distance from the truth) of multi-separators computed by Algorithm 2 for volume images of **filaments** (top) and Algorithm 1 for volume images of **foam cells** (bottom) with five amounts of noise t (columns), as a function of the bias b . Depicted are the VI-WS (red) as well as the conditional entropies due to false cuts (FC, green) and false joins (FJ, yellow). Thick lines indicate the median across those images of the data set with the amount of noise t . Shaded areas indicate the second and third quartile. Dashed lines indicate the 0.1 and 0.9-quantile.

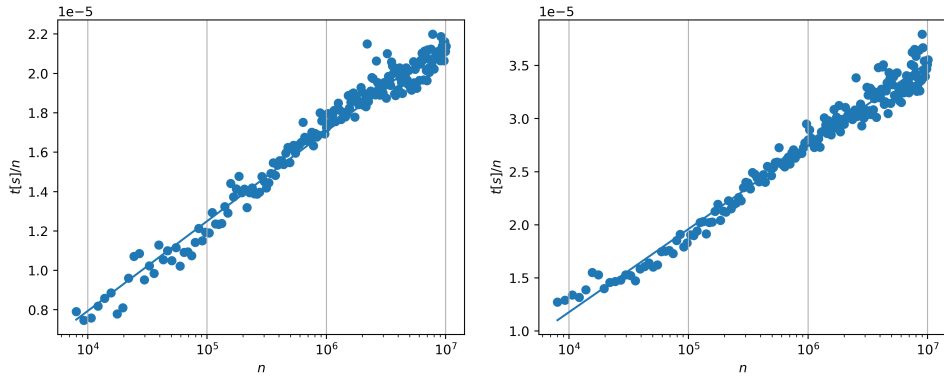


Figure 13: Depicted on the left is the runtime per voxel of our single-thread C++ implementation of Algorithm 1 for instances of the multi-separator problem from volume images of **foam cells**. Depicted on the right is the runtime per voxel of our single-thread C++ implementation of Algorithm 2 for instances of the multi-separator problem from volume images of **filaments**. Both are for volume images of $n = m \times m \times m$ voxels, with $m \in \{20, \dots, 216\}$, synthesized as described in Section 5.1 and Appendix A.1, with the noise level $t = 0.5$ and bias $b = 0$.

by Algorithms 1 and 2 are not sensitive to small deviations of the bias b from the optimum (Figure 12, Columns 1 to 3). For $t > 0.5$, multi-separators output by Algorithms 1 and 2 can still be significantly closer to the truth than those output by the watershed algorithm in terms of the distance VI-WS (Figures 10 and 11, left). However, the sensitivity of the multi-separators output by Algorithms 1 and 2 to the choice of the bias b increases with increasing noise (Figure 12, Columns 4 and 5). For $t = 1$, all multi-separators output by any of the algorithms are inaccurate.

A negative bias b generally leads to more false cuts and less false joins (Figure 12). The optimal bias does not differ much across multiple volume images exhibiting the same amount of noise. This can be seen from Figure 12 where the area within the 0.1 and 0.9 quantile is small.

For instances of the multi-separator problem that witnessed the worst case time complexities established in Lemmas 2 and 3, Algorithms 1 and 2 would not be practical. For the instances we consider here, however, we observe an empirical runtime of approximately $\mathcal{O}(|V| \log |V|)$, for both algorithms (Figure 13).

5.7.2 Specific observations for filaments

For volume images of filaments, segmentations are prone to false cuts: If the gray values of just a few voxels on a filament are distorted due to noise, *locally* it may appear as if there were two distinct filaments. By modeling the segmentation task as a multi-separator problem with attractive *long-range* interactions, it is possible to avoid false cuts due to such local distortions (Figure 10, bottom center). Only for large amounts of noise ($t \geq 0.8$) do the multi-separators output by Algorithm 2 suffer from false cuts and false joins of filaments (Figure 10 bottom).

The watershed algorithm computes multi-separators with the least inaccuracy for $\theta_{\text{start}} \approx \theta_{\text{end}}$ (Figure 15 in Appendix A.3). Smaller values of θ_{start} can lead to multiple distinct seeds for one filament and thus to false cuts (Figure 15, middle row). Greater values of θ_{end} can lead to a later termination of the flood-filling procedure, which leads to thicker filaments and thus to false joins (Figure 15, bottom row). Moreover, a large value of θ_{start} leads to many voxels falsely output by the watershed algorithm as non-separator, which causes false joins (Figure 10 top right and Figure 8 fourth column). These effects are one reason why fundamentally different techniques are used for reconstructing filaments (cf. Section 2).

Numerical results corresponding to the examples depicted in Figure 8 are reported in Table 1 in Appendix A.2. For noise $t = 0.5$, for instance, the multi-separator computed by Algorithm 2 has distance VI-WS = 0.144 from the truth, with FC = 0.059 and FJ = 0.084 while the multi-separator output by the watershed algorithm has distance VI-WS = 0.250 from the truth, with FC = 0.075 and FJ = 0.174. For greater levels of noise, the quantitative difference between the multi-separators output by the watershed algorithm and Algorithm 2 is also reflected in the variation of information with respect to non-separator voxels. For instance, for $t = 0.75$, the multi-separator computed by Algorithm 2 has VI-NS = 0 due to no false cuts or joins of filaments. In contrast, the multi-separator output by the watershed algorithm has VI-NS = 0.435 due to false cuts of some filaments (green and red filaments in row 4 column 4 of Figure 8).

5.7.3 Specific observations for foam cells

For volume images of foam cells, segmentations are prone to false joins: If the gray values of just a few voxels on a membrane are distorted due to noise, *locally* it may appear as if the two cells that are separated by that membrane are one cell. By modeling the segmentation task as a multi-separator problem involving also *long-range* interactions, it is possible to avoid false cuts due to such local distortions (Figure 11, bottom right). Only for large amounts of noise ($t \geq 0.8$) do the multi-separators output by Algorithm 1 suffer from false cuts and false joins of foam cells (Figure 11 bottom).

For the watershed algorithm, there are two regions for the parameters θ_{start} and θ_{end} for which multi-separators with the least inaccuracy are computed for foam cells (Figure 16 in Appendix A.3): In order for the watershed algorithm to avoid false cuts, there needs to be exactly one seed region per foam cell. This can be archived by either large $\theta_{\text{start}} \approx 0.4$ which ideally leads to one large

seed per foam cell, or by small $\theta_{\text{start}} \approx 0.15$ which ideally leads to one small seed per foam cell. Intermediate values for θ_{start} lead to multiple seeds per foam cell which leads to false cuts (Figure 16, middle row). Very small or very large values of θ_{start} lead to false joins (Figure 16, bottom row): If θ_{start} is too small, there need not be a seed in each foam cell. During the flood filling step of the watershed algorithm, the seed from one foam cell can spill into another foam cell that does not have a seed. If θ_{start} is too large, the maximal components of all voxels with a value less than θ_{start} can already cross the membranes. The tradeoff between false cuts and false joins in multi-separators computed by the watershed algorithm can be seen in the second and third column of Figure 11. The parameter θ_{end} determines at which point the flood filling algorithm is terminated. A small θ_{end} leads to an early termination which results in smaller foam cells and thicker membrane while a large θ_{end} leads to a late termination which results in larger foam cells and a thinner membrane. Too thin or thick membranes are penalized by the VI-WS (as this results in too few or too many singleton sets in the computation of the VI-WS).

Numerical results corresponding to the examples depicted in Figure 9 are reported in Table 2 in Appendix A.2. For noise $t = 0.5$, for instance, the multi-separator computed by Algorithm 1 has distance VI-WS = 1.400, with FC = 0.970 and FJ = 0.430, while the multi-separator output by the watershed algorithm has distance VI-WS = 2.110 from the truth, with FC = 1.281 and FJ = 0.828. The variation of information with respect to non-separator voxels is VI-NS = 0.023 with FC-NS = 0.022 and FJ-NS = 0.001 for the multi-separator computed by Algorithm 1 and VI-NS = 0.671 with FC-NS = 0.283 and FJ-NS = 0.388 for multi-separator computed by the watershed algorithm. The low VI-NS value for the multi-separator computed by Algorithm 1 indicates that there are very few false cuts and false joins of foam cells. The higher VI-WS value is a consequence of individual voxels wrongly identified as separator/non-separator. In contrast, the multi-separator output by the watershed algorithm suffers from false cuts (gray segments in Row 3 Column 4 of Figure 9) and false joins (segments in bottom center and top right in Row 3 Column 4 of Figure 9) of foam cells as well as voxels that are wrongly identified as separator/non-separator.

The greedy separator shrinking algorithm (Algorithm 1) has a bias toward removing nodes from the separator that are adjacent to nodes that are not in the separator, instead of removing nodes from the separator whose neighbors are also part of the separator: By the greedy paradigm, the node whose removal from the separator decreases the total cost maximally is removed. If all neighbors of a node are in the separator, then, removing that node from the separator leaves all interactions adjacent to that node separated, i.e. the total cost is only changed by the cost of that node. Otherwise, the total cost is changed by the cost of that node *and* the cost of all interactions that are no longer separated. Such a bias is not unique to Algorithm 1 for the multi-separator problem but it also exists for greedy contraction based algorithms for the (lifted) multicut problem, like GAEC (Keuper et al., 2015).

In the context of segmenting foam cells, this bias can result in the algorithm finding poor local optima for the following reason: Once a node is removed from the separator, the described bias leads to neighboring nodes being more likely to be removed next. The result can be that the component corresponding to one foam cell is growing before a component corresponding to a different foam is started. Consequently, it can happen that the component corresponding to one foam cell grows beyond its membrane because there does not yet exist a component corresponding to a neighboring foam cell (the existence of a component corresponding to a neighboring foam cell would result in a penalty for removing a node from the separator between the two components as many repulsive interactions between these components would no longer be separated). This ultimately leads to false joins in the computed separator. In our experiments, this behavior manifests only for low amounts of noise ($t \leq 0.2$) as can be seen from Figure 11 (bottom right). Moreover, it can be overcome easily, by starting Algorithm 1 not with all but with most nodes in the separator, e.g. those 90% of the nodes with the lowest cost. For consistency, we do not implement such heuristics and only report results for Algorithm 1 initialized with all nodes in the separator.

6 Conclusion

We have introduced the multi-separator problem, a combinatorial optimization problem with applications to the task of image segmentation. While the general problem is NP-hard and even hard to approximate, we have identified two special cases of the objective function for which the problem can be solved efficiently. For the general NP-hard case, we have defined two efficient local search algorithms. In experiments with synthetic volume images of simulated filaments and foam cells, we have seen for all but extreme amounts of noise, that the multi-separator problem in connection with Algorithms 1 and 2 can result in significantly more accurate segmentations than a watershed algorithm, with a practical runtime. For moderate noise, these segmentations are not sensitive to small biases in objective function of the multi-separator problem, as long as the bias is positive, for filaments, and negative, for foam cells. Given the popularity of the watershed algorithm for segmenting foam cells, and given that, so far, fundamentally different models and algorithms are used for segmenting filaments, (cf. Section 2), the multi-separator problem contributes to a more symmetric treatment of these extreme cases of the image segmentation task and holds promise for volume images in which both structures are present, e.g., for volume images of nervous systems acquired in the field of connectomics (Lee et al., 2021).

The results of this work motivate further studies of the multi-separator problem both theoretically and in connection with practical applications. Theoretical questions concern, e.g., the complexity and approximability of the problem for special classes of graphs. Specifically, planar graphs are of interest in the context of segmenting 2-dimensional images. Also of interest are exact algorithms for the multi-separator problem. To this end, the problem can be stated in the form of an integer linear program which then can be solved by a branch and cut algorithm. Studying the polytope associated with the set of feasible solutions of the integer linear program will be of interest to improve exact and approximate algorithms. Another open problem asks for an efficient implementation of a local search algorithm that adds and removes nodes from the separator. To realize such an algorithm, findings on the dynamic connectivity problem (Holm et al., 2001) can be considered.

References

- Amir Alush and Jacob Goldberger. Hierarchical image segmentation using correlation clustering. *IEEE Trans. Neural Networks Learn. Syst.*, 27(6):1358–1367, 2016. doi: 10.1109/TNNLS.2015.2505181.
- Bjoern Andres, Jörg Hendrik Kappes, Thorsten Beier, Ullrich Köthe, and Fred A Hamprecht. Probabilistic image segmentation with closedness constraints. In *ICCV*, 2011. doi: 10.1109/ICCV.2011.6126550.
- Bjoern Andres, Silvia Di Gregorio, Jannik Irmay, and Jan-Hendrik Lange. A polyhedral study of lifted multicuts. *Discrete Optimization*, 47:100757, 2023. doi: 10.1016/j.disopt.2022.100757.
- Phipps Arabie and Scott A. Boorman. Multidimensional scaling of measures of distance between partitions. *Journal of Mathematical Psychology*, 10(2):148–203, 1973. doi: 10.1016/0022-2496(73)90012-6.
- Yoram Bachrach, Pushmeet Kohli, Vladimir Kolmogorov, and Morteza Zadimoghaddam. Optimal coalition structure generation in cooperative graph games. In *AAAI*, 2013. doi: 10.1609/aaai.v27i1.8653.
- Egon Balas and Cid Carvalho de Souza. The vertex separator problem: a polyhedral investigation. *Mathematical Programming*, 103(3):583–608, 2005. doi: 10.1007/s10107-005-0574-7.
- Nikhil Bansal, Avrim Blum, and Shuchi Chawla. Correlation clustering. *Machine learning*, 56: 89–113, 2004. doi: 10.1023/B:MACH.0000033116.57574.95.

- Francisco Barahona. On the computational complexity of Ising spin glass models. *Journal of Physics A: Mathematical and General*, 15(10):3241, 1982. doi: 10.1088/0305-4470/15/10/028.
- Thorsten Beier, Thorben Kroeger, Jörg Hendrik Kappes, Ullrich Köthe, and Fred A. Hamprecht. Cut, glue & cut: A fast, approximate solver for multicut partitioning. In *CVPR*, 2014. doi: 10.1109/CVPR.2014.17.
- Thorsten Beier, Fred A. Hamprecht, and Jörg Hendrik Kappes. Fusion moves for correlation clustering. In *CVPR*, 2015. doi: 10.1109/CVPR.2015.7298973.
- Thorsten Beier, Constantin Pape, Nasim Rahaman, Timo Prange, Stuart Berg, Davi D. Bock, Albert Cardona, Graham W. Knott, Stephen M. Plaza, Louis K. Scheffer, et al. Multicut brings automated neurite segmentation closer to human performance. *Nature methods*, 14(2):101–102, 2017. doi: 10.1038/nmeth.4151.
- Anne Berry, Jean-Paul Bordat, and Olivier Cogis. Generating all the minimal separators of a graph. *International Journal of Foundations of Computer Science*, 11(03):397–403, 2000. doi: 10.1142/S0129054100000211.
- Moses Charikar, Venkatesan Guruswami, and Anthony Wirth. Clustering with qualitative information. *Journal of Computer and System Sciences*, 71(3):360–383, 2005. doi: 10.1016/j.jcss.2004.10.012.
- Sunil Chopra and Mendu R. Rao. The partition problem. *Mathematical programming*, 59(1-3): 87–115, 1993. doi: 10.1007/BF01581239.
- Denis Cornaz, Fabio Furini, Mathieu Lacroix, Enrico Malaguti, A. Ridha Mahjoub, and Sébastien Martin. The vertex k-cut problem. *Discrete Optimization*, 31:8–28, 2018. doi: 10.1016/j.disopt.2018.07.003.
- Denis Cornaz, Youcef Magnouche, Ali Ridha Mahjoub, and Sébastien Martin. The multi-terminal vertex separator problem: Polyhedral analysis and branch-and-cut. *Discrete Applied Mathematics*, 256:11–37, 2019. doi: 10.1016/j.dam.2018.10.005.
- Erik D. Demaine, Dotan Emanuel, Amos Fiat, and Nicole Immorlica. Correlation clustering in general weighted graphs. *Theoretical Computer Science*, 361(2-3):172–187, 2006. doi: 10.1016/j.tcs.2006.05.008.
- Mohamed Didi Biha and Marie-Jean Meurs. An exact algorithm for solving the vertex separator problem. *Journal of Global Optimization*, 49:425–434, 2011.
- Fernando Escalante. Schnittverbände in Graphen. *Abh.Math.Semin.Univ.Hambg.*, 38:199–220, 1972. doi: 10.1007/BF02996932.
- Junichiro Fukuyama. NP-completeness of the planar separator problems. *J. Graph Algorithms Appl.*, 10(2):317–328, 2006. doi: 10.7155/jgaa.00130.
- Fabio Furini, Ivana Ljubić, Enrico Malaguti, and Paolo Paronuzzi. On integer and bilevel formulations for the k-vertex cut problem. *Mathematical Programming Computation*, 12:133–164, 2020. doi: 10.1007/s12532-019-00167-1.
- Naveen Garg, Vijay V. Vazirani, and Mihalis Yannakakis. Multiway cuts in directed and node weighted graphs. In *ICALP*, 1994. doi: 10.1007/3-540-58201-0_92.
- Naveen Garg, Vijay V. Vazirani, and Mihalis Yannakakis. Multiway cuts in node weighted graphs. *Journal of Algorithms*, 50(1):49–61, 2004. doi: 10.1016/S0196-6774(03)00111-1.
- Martin Grötschel, László Lovász, and Alexander Schrijver. The ellipsoid method and its consequences in combinatorial optimization. *Combinatorica*, 1(2):169–197, 1981. doi: 10.1007/BF02579273.

- Jacob Holm, Kristian De Lichtenberg, and Mikkel Thorup. Poly-logarithmic deterministic fully-dynamic algorithms for connectivity, minimum spanning tree, 2-edge, and biconnectivity. *Journal of the ACM (JACM)*, 48(4):723–760, 2001. doi: 10.1145/502090.502095.
- John Hopcroft and Robert Tarjan. Algorithm 447: efficient algorithms for graph manipulation. *Communications of the ACM*, 16(6):372–378, 1973. doi: 10.1145/362248.362272.
- Andrea Hornáková, Jan-Hendrik Lange, and Bjoern Andres. Analysis and optimization of graph decompositions by lifted multicuts. In *ICML, 2017*. URL <https://proceedings.mlr.press/v70/hornakova17a.html>.
- Andrea Hornáková, Roberto Henschel, Bodo Rosenhahn, and Paul Swoboda. Lifted disjoint paths with application in multiple object tracking. In *ICML, 2020*. URL <http://proceedings.mlr.press/v119/hornakova20a.html>.
- Jörg Hendrik Kappes, Markus Speth, Bjoern Andres, Gerhard Reinelt, and Christoph Schnörr. Globally optimal image partitioning by multicuts. In *EMMCVPR, 2011*. doi: 10.1007/978-3-642-23094-3_3.
- Jörg Hendrik Kappes, Markus Speth, Gerhard Reinelt, and Christoph Schnörr. Higher-order segmentation via multicuts. *Computer Vision and Image Understanding*, 143:104–119, 2016a. doi: 10.1016/j.cviu.2015.11.005.
- Jörg Hendrik Kappes, Paul Swoboda, Bogdan Savchynskyy, Tamir Hazan, and Christoph Schnörr. Multicuts and perturb & MAP for probabilistic graph clustering. *J. Math. Imaging Vis.*, 56(2): 221–237, 2016b. doi: 10.1007/s10851-016-0659-3.
- Amirhossein Kardoost and Margret Keuper. Solving minimum cost lifted multicut problems by node agglomeration. In *ACCV, 2018*. doi: 10.1007/978-3-030-20870-7_5.
- Amirhossein Kardoost and Margret Keuper. Uncertainty in minimum cost multicuts for image and motion segmentation. In *UAI, 2021*. URL <https://proceedings.mlr.press/v161/kardoost21a.html>.
- Richard Manning Karp. Reducibility among combinatorial problems. In *Complexity of computer computations*, 1972. doi: 10.1007/978-1-4684-2001-2_9.
- Margret Keuper. Higher-order minimum cost lifted multicuts for motion segmentation. In *ICCV, 2017*. doi: 10.1109/ICCV.2017.455.
- Margret Keuper, Evgeny Levinkov, Nicolas Bonneel, Guillaume Lavoué, Thomas Brox, and Bjoern Andres. Efficient decomposition of image and mesh graphs by lifted multicuts. In *ICCV, 2015*. doi: 10.1109/ICCV.2015.204.
- Sungwoong Kim, Chang Dong Yoo, Sebastian Nowozin, and Pushmeet Kohli. Image segmentation using higher-order correlation clustering. *IEEE Trans. Pattern Anal. Mach. Intell.*, 36(9): 1761–1774, 2014. doi: 10.1109/TPAMI.2014.2303095.
- Alexander Kirillov, Evgeny Levinkov, Bjoern Andres, Bogdan Savchynskyy, and Carsten Rother. InstanceCut: from edges to instances with multicut. In *CVPR, 2017*. doi: 10.1109/CVPR.2017.774.
- Philip N. Klein, Claire Mathieu, and Hang Zhou. Correlation clustering and two-edge-connected augmentation for planar graphs. *Algorithmica*, pages 1–34, 2023. doi: 10.1007/s00453-023-01128-w.
- Kisuk Lee, Ran Lu, Kyle Luther, and Hyunjune Sebastian Seung. Learning and segmenting dense voxel embeddings for 3d neuron reconstruction. *IEEE Transactions on Medical Imaging*, 40(12): 3801–3811, 2021. doi: 10.1109/TMI.2021.3097826.
- Richard Jay Lipton and Robert Endre Tarjan. A separator theorem for planar graphs. *SIAM Journal on Applied Mathematics*, 36(2):177–189, 1979. doi: 10.1137/0136016.

- Youcef Magnouche, Ali Ridha Mahjoub, and Sébastien Martin. The multi-terminal vertex separator problem: Branch-and-cut-and-price. *Discrete Applied Mathematics*, 290:86–111, 2021. doi: 10.1016/j.dam.2020.06.021.
- Marina Meilă. Comparing clusterings—an information based distance. *Journal of Multivariate Analysis*, 98(5):873–895, 2007. doi: 10.1016/j.jmva.2006.11.013.
- Karl Menger. Zur allgemeinen Kurventheorie. *Fundamenta Mathematicae*, 10(1):96–115, 1927. URL <http://eudml.org/doc/211191>.
- Fernand Meyer. Un algorithme optimal pour la ligne de partage des eaux. In *8e congrès de reconnaissance des formes et intelligence artificielle*, 1991.
- Shervin Minaee, Yuri Boykov, Fatih Porikli, Antonio Plaza, Nasser Kehtarnavaz, and Demetri Terzopoulos. Image segmentation using deep learning: A survey. *IEEE Transactions on Pattern Analysis and Machine Intelligence*, 44(7):3523–3542, 2022. doi: 10.1109/TPAMI.2021.3059968.
- Anna Moss and Yuval Rabani. Approximation algorithms for constrained node weighted Steiner tree problems. *SIAM Journal on Computing*, 37(2):460–481, 2007. doi: 10.1137/S0097539702420474.
- Sebastian Nowozin and Christoph H. Lampert. Global interactions in random field models: A potential function ensuring connectedness. *SIAM J. Imaging Sci.*, 3(4):1048–1074, 2010. doi: 10.1137/090752614.
- Markus Rempfler, Matthias Schneider, Giovanna D. Ielacqua, Xianghui Xiao, Stuart R. Stock, Jan Klohs, Gbor Székely, Bjoern Andres, and Bjoern H. Menze. Reconstructing cerebrovascular networks under local physiological constraints by integer programming. *Medical Image Analysis*, 25(1):86–94, 2015. doi: 10.1016/j.media.2015.03.008.
- Jos B.T.M. Roerdink and Arnold Meijster. The watershed transform: Definitions, algorithms and parallelization strategies. *Fundamenta informaticae*, 41(1-2):187–228, 2000. doi: 10.3233/FI-2000-411207.
- Suprosanna Shit, Rajat Koner, Bastian Wittmann, Johannes C. Paetzold, Ivan Ezhov, Hongwei Li, Jiazhen Pan, Sahand Sharifzadeh, Georgios Kaissis, Volker Tresp, and Bjoern H. Menze. Relationformer: A unified framework for image-to-graph generation. In *ECCV*, 2022. doi: 10.1007/978-3-031-19836-6_24.
- Cid Carvalho de Souza and Egon Balas. The vertex separator problem: algorithms and computations. *Mathematical Programming*, 103(3):609–631, 2005. doi: 10.1007/s10107-005-0573-8.
- Siyu Tang, Mykhaylo Andriluka, Bjoern Andres, and Bernt Schiele. Multiple people tracking by lifted multicut and person re-identification. In *CVPR*, 2017. doi: 10.1109/CVPR.2017.394.
- Engin Türetken, Fethallah Benmansour, Bjoern Andres, Przemyslaw Glowacki, Hanspeter Pfister, and Pascal Fua. Reconstructing curvilinear networks using path classifiers and integer programming. *IEEE Trans. Pattern Anal. Mach. Intell.*, 38(12):2515–2530, 2016. doi: 10.1109/TPAMI.2016.2519025.
- Stéfan van der Walt, Johannes L. Schönberger, Juan Nunez-Iglesias, François Boulogne, Joshua D. Warner, Neil Yager, Emmanuelle Gouillart, Tony Yu, and the scikit-image contributors. scikit-image: image processing in Python. *PeerJ*, 2:e453, 6 2014. doi: 10.7717/peerj.453.
- Luc Vincent and Pierre Soille. Watersheds in digital spaces: an efficient algorithm based on immersion simulations. *IEEE Trans. Pattern Anal. Mach. Intell.*, 13(6):583–598, 1991. doi: 10.1109/34.87344.
- Thomas Voice, Maria Polukarov, and Nicholas R. Jennings. Coalition structure generation over graphs. *Journal of Artificial Intelligence Research*, 45:165–196, 2012. doi: 10.1613/jair.3715.

Steffen Wolf, Alberto Bailoni, Constantin Pape, Nasim Rahaman, Anna Kreshuk, Ullrich Köthe, and Fred A. Hamprecht. The mutex watershed and its objective: Efficient, parameter-free graph partitioning. *IEEE Trans. Pattern Anal. Mach. Intell.*, 43(10):3724–3738, 2020. doi: 10.1109/TPAMI.2020.2980827.

Julian Yarkony, Alexander Ihler, and Charless C. Fowlkes. Fast planar correlation clustering for image segmentation. In *ECCV*, 2012. doi: 10.1007/978-3-642-33783-3_41.

Chong Zhang, Julian Yarkony, and Fred A. Hamprecht. Cell detection and segmentation using correlation clustering. In *MICCAI*, 2014. doi: 10.1007/978-3-319-10404-1_2.

A Appendix

A.1 Volume image synthesis (details)

In order to synthesize binary volume images of filaments, we draw n cubic splines randomly so as to intersect the unit cube and such that the minimal distance between any two splines is at least d_{\min} . Regarding the parameters of the splines, regarding the distributions from which these parameters are drawn, and regarding the rejection of splines that violate the constraints, we refer the reader to the supplementary C++ code. Then, considering the canonical embedding of the 3-dimensional grid graph of $m \times m \times m$ voxels in the unit cube, we label voxels 0 if and only if their Euclidean distance in the unit cube to the nearest spline is at most r . In our experiments, $m = 64$, $d_{\min} = \frac{10}{m}$ and $r = \frac{0.75}{m}$. Thus, the center lines of the filaments are at least 10 voxels apart, and the filaments have a width of 1.5 voxels.

In order to synthesize binary volume images of foam cells, we draw n pairwise non-neighboring voxels uniformly at random from the $m \times m \times m$ voxel grid graph. These voxels are labeled $1, \dots, n$, respectively. All other voxels are labeled 0. Next, we repeat the following randomized region growing procedure until termination: We draw a voxel v uniformly at random from the set of voxels w that hold three properties: (i) w is labeled 0, (ii) there is a non-zero label among the labels of the neighbors w , and (iii) this non-zero label is unique, called i_w . If no such voxel exists, the procedure terminates. Otherwise, v is labeled i_v . This results in a voxel labeling such that, for every non-zero label i , the set of voxels labeled i induces a component of the voxel grid graph, and these components are separated by the set of voxels labeled 0. Next, we erode the components of voxels with a non-zero label with a spherical kernel of radius $\frac{d_{\min}}{2} + r$. In our experiments, $m = 64$, $d_{\min} = 8$ and $r = 0.75$. If this erosion disconnects voxels with the same non-zero label, we label 0 all except one maximal component of such voxels. Next, we again grow components of voxels with a non-zero label, now deterministically by breath-first search, until all voxels labeled 0 are adjacent to at last two voxels with distinct non-zero labels. Then, we label 0 also all voxels with a Euclidean distance of at most r to any voxel labeled 0. This ensures that all components of voxels with a non-zero label (to-become foam cells) are separated by a $2r$ -wide set of voxels labeled 0 (to-become cell membranes). Finally, we obtain a binary image by labeling 1 precisely those voxels whose integer label is 0.

To obtain gray scale images from the binary images described above, we proceed as follows: For images of filaments, we compute the distance from each voxel to the nearest spline. For images of foam cells, we compute the distance from each voxel to the nearest membrane, more specifically, to the nearest voxel labeled 0 during the synthesis of the binary image, at the end of the breadth-first search. Let d be this distance for a given voxel v . We define the gray value of v as $g = w(d)g_1 + (1 - w(d))g_2$, clipped to the interval $[0, 1]$. Here, g_1 and g_2 are samples from two normal distribution with means and standard deviations μ_1, σ_1 and μ_2, σ_2 , and g is a weighted sum with the weight $w(d)$ depending on the distance d according to the function written below that is depicted in Figure 14:

$$w(d) = \frac{1}{1 + \left(\frac{w_{\max}}{1 - w_{\max}}\right)^{d/r - 1}} \quad \text{with} \quad w_{\max} \in \left(\frac{1}{2}, 1\right)$$

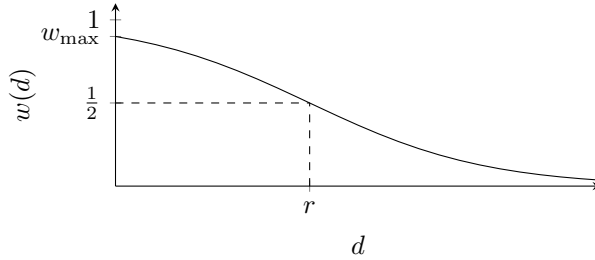


Figure 14: Depicted above its the weight w as a function of the distance d .

t	Alg.	θ_{start}	θ_{end}	b	VI-WS	FC	FJ	VI-NS	FC-NS	FJ-NS
0.00	WS	0.580	0.580		0.056	0.008	0.048	0.000	0.000	0.000
	MS			0.06	0.054	0.007	0.046	0.000	0.000	0.000
0.25	WS	0.580	0.585		0.104	0.022	0.082	0.000	0.000	0.000
	MS			0.09	0.079	0.013	0.065	0.000	0.000	0.000
0.50	WS	0.580	0.580		0.250	0.075	0.174	0.000	0.000	0.000
	MS			0.08	0.144	0.059	0.084	0.000	0.000	0.000
0.75	WS	0.570	0.570		0.750	0.421	0.330	0.435	0.435	0.000
	MS			0.01	0.406	0.317	0.089	0.000	0.000	0.000
1.00	WS	0.555	0.565		1.447	0.781	0.666	1.045	0.907	0.138
	MS			-0.11	1.345	1.274	0.071	0.749	0.749	0.000

Table 1: This table summarizes the numerical results corresponding to the renderings in Figure 8 for **filaments**. For the watershed algorithm (WS) the thresholds θ_{start} and θ_{end} , and for the multi-separator (MS) algorithm the biases are chosen so as to minimize the average VI-WS across those images of the data set with the amount of noise t .

This function decreases monotonically such that $w(0) = w_{\text{max}}$ and $w(r) = \frac{1}{2}$, and $w(d) \rightarrow 0$ for $d \rightarrow \infty$. In our experiments, $w_{\text{max}} = 0.9$. For μ_1, σ_1, μ_2 , and σ_2 , we consider different numbers in order to vary the amount of noise, and thus, the difficulty of reconstructing the binary image from the gray scale image. More specifically, we define $\mu_1^{\text{start}}, \mu_1^{\text{end}}, \sigma_1^{\text{start}}, \sigma_1^{\text{end}}, \mu_2^{\text{start}}, \mu_2^{\text{end}}, \sigma_2^{\text{start}}, \sigma_2^{\text{end}}$, and for the parameter $t \in [0, 1]$: $\mu_i = (1 - t)\mu_i^{\text{start}} + t(\mu_i^{\text{end}})$ and $\sigma_i = (1 - t)\sigma_i^{\text{start}} + t(\sigma_i^{\text{end}})$ for $i = 1, 2$. For filaments, $\mu_1^{\text{start}} = 0.3, \mu_1^{\text{end}} = 0.38, \mu_2^{\text{start}} = 0.7, \mu_2^{\text{end}} = 0.62, \sigma_1^{\text{start}} = \sigma_2^{\text{start}} = 0.05, \sigma_1^{\text{end}} = \sigma_2^{\text{end}} = 0.1$. For foam cells, $\mu_1^{\text{start}} = 0.7, \mu_1^{\text{end}} = 0.55, \mu_2^{\text{start}} = 0.3, \mu_2^{\text{end}} = 0.45, \sigma_1^{\text{start}} = \sigma_2^{\text{start}} = 0.05, \sigma_1^{\text{end}} = \sigma_2^{\text{end}} = 0.1$. These parameters are chosen such that voxels labeled 1 in the binary image will, in expectation, be brighter than voxels labeled 0 in the binary image. Moreover, the parameters are chosen such that, for $t = 0$, all algorithms we consider output near perfect reconstructions of the binary images, and, for $t = 1$, all algorithms we consider output binary images with severe mistakes.

A.2 Detailed numerical results for renderings

Table 1 and Table 2 report the numerical results corresponding to the examples that are depicted in Figure 8 and Figure 9, respectively.

A.3 Analysis of parameters of watershed algorithm

Figures 15 and 16 depict the inaccuracy of multi-separators computed by the watershed algorithm for volume images of filaments and foam cells, respectively.

t	Alg.	θ_{start}	θ_{end}	b	VI-WS	FC	FJ	VI-NS	FC-NS	FJ-NS
0.00	WS	0.380	0.470		0.566	0.421	0.144	0.023	0.023	0.000
	MS			-0.10	0.480	0.354	0.126	0.000	0.000	0.000
0.25	WS	0.390	0.470		1.083	0.787	0.296	0.209	0.101	0.108
	MS			-0.08	0.769	0.535	0.234	0.005	0.005	0.000
0.50	WS	0.120	0.480		2.110	1.281	0.828	0.671	0.283	0.388
	MS			-0.03	1.400	0.970	0.430	0.023	0.022	0.001
0.75	WS	0.120	0.470		3.273	2.540	0.734	0.657	0.472	0.185
	MS			0.06	2.552	1.565	0.987	0.085	0.080	0.005
1.00	WS	0.430	0.600		4.526	2.810	1.716	3.275	1.941	1.334
	MS			0.17	4.769	2.504	2.265	1.586	0.674	0.912

Table 2: This table summarizes the numerical results corresponding to the renderings in Figure 9 for **foam cells**. For the watershed algorithm (WS) the thresholds θ_{start} and θ_{end} , and for the multi-separator (MS) algorithm the biases are chosen so as to minimize the average VI-WS across those images of the data set with the amount of noise t .

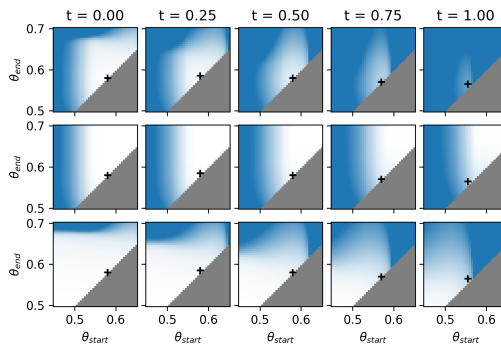


Figure 15: Depicted above is the inaccuracy (distance from truth) of multi-separators computed by the watershed algorithm (Section 5.3) for volume images of **filaments** with five amounts of noise t (columns) for all values of θ_{start} (x-axis) and θ_{end} (y-axis). The three rows depict the medians across those images of the data set with the amount of noise t of the VI-WS (top) and the conditional entropies due to false cuts (FC, middle) and false joins (FJ, bottom). White indicates a value of 0 and saturated blue indicates a value of 2 or greater. Infeasible parameters (i.e. $\theta_{\text{start}} > \theta_{\text{end}}$) are depicted in gray. The + symbol indicates the parameters that archive the best median VI-WS.

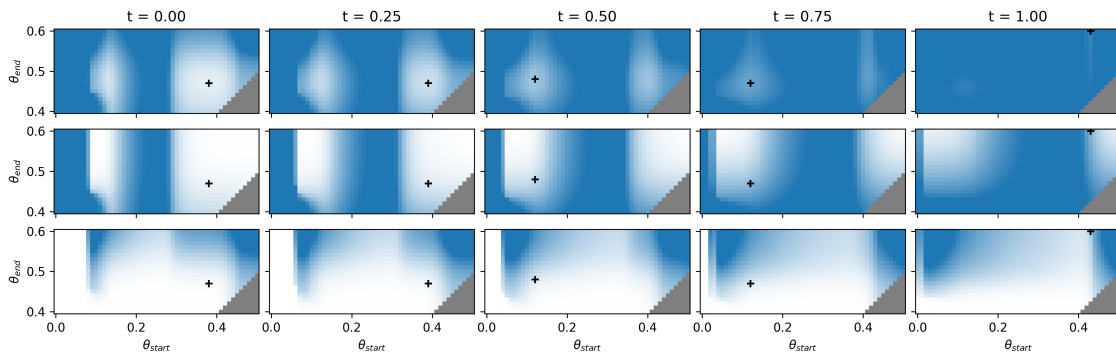


Figure 16: Depicted above is the inaccuracy (distance from truth) of multi-separators computed by the watershed algorithm (Section 5.3) for volume images of **foam cells** completely analogous to Figure 15.